ABSTRACT

Title of Document: ZONE MODELING OF VERY-LOW-FREQUENCY UNSTABLE BEHAVIOR IN MECHANICALLY-VENTILATED COMPARTMENT FIRES

Xiaoyue Pi, Master of Science, 2015

Directed By: Professor Arnaud Trouvé
Department of Fire Protection Engineering

A zone model is developed to simulate the oscillatory behavior occasionally observed in compartment fires. This oscillatory behavior is the result of an unstable coupling between the liquid fuel evaporation rate, the combustion process, the compartment pressure and the ventilation of the compartment. The governing equations use a classical zone modeling approach combined with a (N-τ) model description of the variations of the fuel evaporation rate. The equations are solved with an in-house Matlab solver. The model is evaluated by comparisons with experimental data previously obtained at Institut de Radioprotection et de Sûreté Nucléaire (IRSN) in France. Three different variations of the (N-τ) model are evaluated, corresponding to a coupling between liquid fuel evaporation and bulk oxygen, bulk temperature or admission flow rate. It is found that the variation corresponding to a coupling between liquid fuel evaporation and bulk oxygen provides the more realistic results.

ZONE MODELING OF VERY-LOW-FREQUENCY UNSTABLE BEHAVIOR IN MECHANICALLY-VENTILATED COMPARTMENT FIRES

By

Xiaoyue Pi

Thesis submitted to the Faculty of the Graduate School of the
University of Maryland, College Park, in partial fulfillment
of the requirements for the degree of
Master of Science
2015

Advisory Committee:
Professor Arnaud Trouvé, Chair
Professor Stanislav Stoliarov
Professor Michael Gollner

Acknowledgements

First of all, I would like to thank my family for supporting my study and accompanying with my growth.

I would like to thank all those people who put considerable efforts into this meaningful research project. I specially would like to thank my advisor - Dr. Arnaud Trouvé- for his outstanding intelligence and patient guidance. I would like to thank people in PRISME project and IRSN for the valuable experimental data sources. I would like to thank Benoît for his contributions to this project before and Sylvain for his detailed explanations to the experimental data. I would like to thank Dr. Stanislav Stoliarov and Dr. Michael Gollner for serving on my defense committee and offering me valuable suggestions. I would like to thank Salman Verma, Cong Zhang, Ruolei Ji, Liying Zhu, Mengting Pan and Patrick Welz a lot for your generous help to the thesis's writing, and it is so nice to have your company during my master's study.

Moreover, I would like to thank Dr. James Milke, Prof. Isman, Nicole Hollywood, Sharon Hodgson, Yan Ding, Wei Tang, Haiqing Guo, Xuan Liu, Chad Lannon, Frida Lundström, Raquel Hakes, Paul Anderson, Maria Theodori, Mohammed Alsaeefan and Mark McKinnon in our FPE department. It is so nice to meet you here.

I also would like to thank my sincere friends who are not in FPE department, but really enriching my life.

Table of Contents

List of Tables

List of Figures

1 Introduction

1.1 Background

Fire behaviors in a compartment, for example the unstable behavior, are closely associated with the variations of surrounding conditions. It is found that room fires can be affected by both thermal and ventilation feedback processes [1]. Therefore, it is necessary to study the behaviors, predict their effects on the fire growth, building structure and environment, and take effective actions. Thus, this project develops a zone model to study the oscillatory behavior which is occasionally observed in compartment fires.

1.1.1 Zone modeling of compartment fires

Computational tools, which range from basic hand calculation, through relatively simple zone model, to detailed field model, are usually used for compartment fires study [2]. Zone model is applied to this research without restricting to basic states or considering the complex differences of the fire magnitudes and environmental conditions on various coordinates.

Generally, a compartment fire is characterized in three phases as it is shown in Figure 1-1 [3]. The first phase shows the fire development from the initial ignition to the maximum if no effective suppression actions were taken. For the second phase, there are two typical regimes, one is over-ventilated (fuel lean), and the other is under-ventilated (fuel rich). After the depletion of the oxygen and fuel, the fire comes to the third cooling phase and results in decay. It is noticeable that the condition of

oxygen-fuel ratio impacts on the last two phases a lot; hence, it is important to study the ventilation regimes during compartment fire growth.

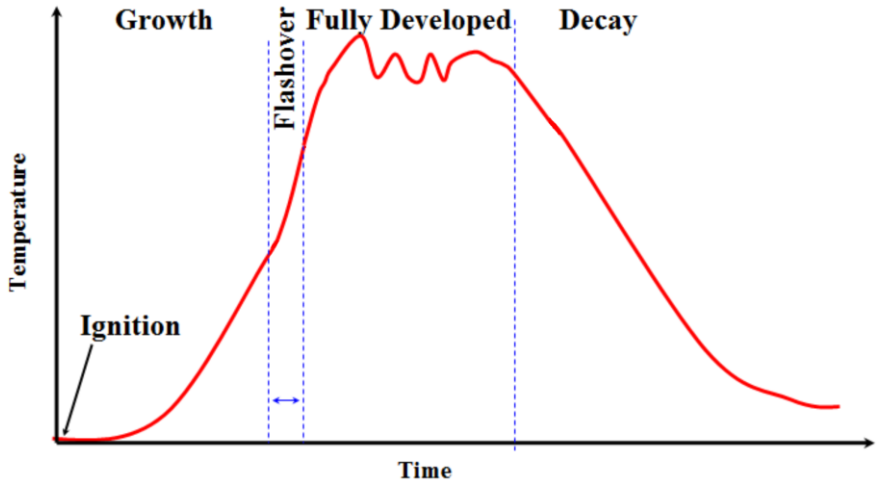

Figure 1-1 Fire development in terms of enclosure temperature

Specially, the compartment in this research is the nuclear plant. Fires in nuclear facilities pose a significant threat to nuclear safety. Generally, a major concern when dealing with safety problems in nuclear facilities is the dynamic confinement to nuclear plants. Therefore, pressure variations effected by the ventilation regimes and oscillatory behaviors in compartments are important to consider.

1.1.2 Ventilation regimes

Both natural and mechanical ventilations are used for the compartment fire experiments and simulations, in order to study the effect of ventilation on the fire development in compartments [4]. Especially, when it is of the under-ventilation regime, the depletion of oxygen may lead the original flame to oscillatory combustion and flame extinction [5]. Therefore, in order to further explore the fire growth, it is important to estimate the degree of the ventilation. This degree can be defined as the actual fuel-to-oxygen ratio to the stoichiometric fuel-to-oxygen ratio as below [6][7]:

$$\phi = \frac{\dfrac{m_{\text{fuel}}}{m_{\text{oxygen}}}}{\left(\dfrac{m_{\text{fuel}}}{m_{\text{oxygen}}}\right)_{\text{stoich}}} \tag{2.1}$$

where ϕ is the degree, named global equivalence ratio. It is noticeable that, if $\phi > 1$, there is extra fuel in the system, therefore, it is a under-ventilated regime; otherwise, if $\phi < 1$, the fuel should be used up during the reaction, therefore, it is an over-ventilated regime.

Furthermore, mechanical ventilation use is preferred to be applied to some specific places where less exposure and special treated are needed, for example, its application to nuclear plants [8].

Various experiments and simulations were done to study the nuclear safety, for instance, Dietmar and Volker [9] worked on a new model to couple heat transfer process during a fire in nuclear plants. It will be further discussed in Section 1.3.3.

1.1.3 Oscillatory behavior

The analysis of the oscillation phenomenon is also vital, since oscillatory behavior is the result of an unstable coupling between the liquid fuel evaporation rate, the combustion process, the compartment pressure and the ventilation of the compartment. Meanwhile, the study of the frequency and amplitude of various oscillations is considered to be helpful to obtain methods for compartment fire's prediction and control.

1.2 Project focus

Fire protection is vital to nuclear plants' safety, and any carelessness or error operations may cause disasters. Therefore, this research focuses on establishing a zone modeling to study the unstable behavior in mechanically-ventilated compartment fires, in order to help improve nuclear plant safety.

The research first uses physics equations which describe the environment conditions, along with Matlab, to establish the numerical model. Zone model instead of field model is applied to this research, since it is a preliminary model without considering the differences on different coordinates.

Furthermore, series of verifications and validations are applied to test the model. Overall, there are two approaches to describe fuel mass loss rate: one is to use designed fire models (prescribed fuel mass loss rates, $\dot{m}_f = \text{function}(t)$), the other is to apply thermal-feedback-sensitive models (simulated fuel mass loss rates, $\dot{m}_f = \text{function}(\dot{q}'') = \text{function}(Y_{O_2}, \bar{T}, \dot{m}_{adm}, \bar{P} \ldots)$). The thermal-feedback-sensitive models are advanced descriptions of fuel pyrolysis, where fires feature a closed-loop heat feedback mechanism and fuel pyrolysis is sensitive to the gas-phase thermal environment. The process of thermal feedback is shown in Figure 1-2 below:

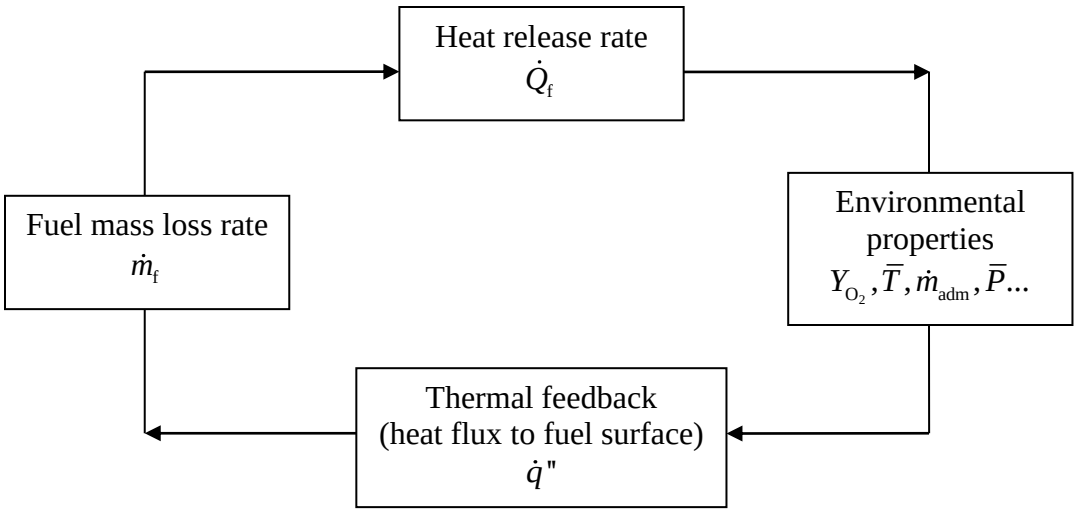

Figure 1-2 A loop of thermal feedback theory

The data sources used for the validations come from the experiments performed by PRISME (French acronym for Fire Propagation in Elementary Multi-room Scenarios) program in Institut de Radioprotection et de Sûreté Nucléaire (IRSN) in France. As PRISME project leader, the IRSN has performed various fire experiments in confined and mechanically-ventilated compartments for nuclear safety study [10]. Two data source packages named PRISME Source D1 and PRISME VSP S3 from them are used in this research for validation.

After that, further oscillation studies are performed by using various coupling results.

1.3 Literature review

1.3.1 Ventilation regimes

An amount of studies on different types of ventilation regimes were performed in the past decades.

According to Sugawa [11] and his group's investigation, the experimental and numerical studies on the over-ventilated cases were more performed at first, since the

amount of oxygen supply is a constant in these cases. For example, the computer codes could be used to simulate fire propagation of over-ventilation regime by using a two-layer zone model. However, in real compartment fire cases, the oxygen supply cannot be enough all the time, since a compartment space is sometimes confined. Therefore, the value of oxygen fraction should vary along with the fire growth, and the original codes need to be developed.

Sugawa [11] et al. studied the methyl alcohol pool fire under the oxygen starvation condition and analyzed the extinction of ghosting fires. Utiskul [12] et al. experimented on the heptane pool fires for an under-ventilation compartment fire regime and found extinction depends on both temperature and oxygen concentration. Except the natural ventilation, mechanical ventilation is also required to be studied due to its wide use and its function to change the environment conditions, for example, the oxygen supply.

There are mainly two modes of mechanical ventilation: one is to push air into the system with positive pressure, the other is to extract air out of the system with negative pressure [13] [14]. Many investigations were done on the mechanical ventilation study, for example, Michelle and Craig [4] pointed out that the forced ventilation regime provide a well-mixed compartment; moreover, they queried the classical assumption that temperature and gas concentration share the same vertical distribution in compartment fires. In addition, in NUREG-1805 [15], the authors pointed out the differences between natural ventilation and mechanical ventilation, which is mainly because the formation of a thermal stratified hot smoke layer in a naturally ventilated room may be disturbed by the ventilation system.

1.3.2 Oscillatory behavior

Decades ago, Takeda and Akita [16] analyzed the behavior of liquid-fuel compartment fires after doing two hundred experiments and concluded that oscillatory combustion plays an important role in compartment fires. Tewarson [17] also found the similar behavior and discussed it in his paper. Utiskul [12] et al. experimented on the heptane pool fires for an under-ventilation compartment fire regime and then noticed the behavior of extinctions and oscillations. In addition, according to Kwang [18] et al.'s experimental study on oscillation behavior in a small-scaled room, the oscillation combustion was found in both stable and unstable combustion regions. Even though it lasted until the fuel was consumed in a stable region, it was followed by extinction in an unstable region.

1.3.3 PRISME project review

Various fire experiments have been performed in the context of the PRISME project in the IRSN facility. Pretrel [19] et al. performed experiments on the fire in confined and ventilated compartment at IRSN. They pointed out the rise or reduction in burning rate is directly linked to pressure variations in the compartment. Pretrel also studied the influence of ventilation procedures on pool fire in a ventilated enclosure with Such [20], and then provided practical solutions about ventilation strategies to limit fire hazards. Le Saux [21] et al. conducted experiments to study the mass loss rate in confined mechanically ventilated multi-room scenarios, and their analyses show that the mass loss rate is dependent on the oxygen concentration and the blow effect towards the pool. Bonte [22] et al. focused on the capability of a zone model (CFAST) and a field model (ISIS), to predict the interaction between mass loss

rate and total relative room pressure or oxygen concentration in case of under-ventilated fire conditions. Models were established by using the mass loss rate that was measured in experiments. Audouin [23] et al. quantified comparisons between various computational results (zone models and field models) and experimental data collected from pool fire scenarios, and concluded the importance to use more than one metric operator for the validations.

2 Zone model formulations

This research applies physics equations to a zone model to simulate compartment fires.

2.1 Conservation laws

When studying compartment fires in this research, the room is considered as a control volume. Therefore, the properties, for example, mass, oxygen fraction and temperature should be noticed in this specific volume. In addition, a zone model instead of a field model is applied in the compartment, that is to say, the differences of the properties among various locations are not concerned. For example, the value of temperature is generally different in various places in the compartment - it is high around the flame but low around the floor; however, it is assumed to be a constant value without considering the exact position in this research. Therefore, the ordinary differential equations (ODE) in Matlab is selected here instead of partial differential equations (PDE).

2.1.1 Conservation of mass

The mass variation in the gas phase control volume is described as the rate of mass coming in as an admission, minus the rate of mass going out as an extraction and plus fuel mass loss rate in the fire:

$$\frac{\mathrm{d}m}{\mathrm{d}t} = \dot{m}_{\mathrm{adm}} - \dot{m}_{\mathrm{ext}} + \dot{m}_{\mathrm{f}} \tag{2.1}$$

where $\frac{\mathrm{d}m}{\mathrm{d}t}$ is the total mass variation in the control volume, $\dot{m}_{\mathrm{adm}}$ is the mass flow rate through the admission duct, $\dot{m}_{\mathrm{ext}}$ is the mass flow rate through the extraction duct, and $\dot{m}_{\mathrm{f}}$ is the fuel mass loss rate in the fire (it will be 0 if there is no fire).

2.1.2 Conservation of mass of oxygen

In the compartment fire, it is important to figure out the mass of air variation along with the time. The reason of focusing on the mass of oxygen is mainly because nitrogen does not impact too much on the compartment environment, neither as water vapor nor carbon dioxide. Therefore, the equation can be expressed as (there is no oxygen coming from the fuel):

$$\frac{\mathrm{d}}{\mathrm{d}t} m_{\mathrm{O_2}} = \dot{m}_{\mathrm{in}} Y_{\mathrm{O_2},\infty} - \dot{m}_{\mathrm{out}} Y_{\mathrm{O_2}} - \dot{\Omega}_{\mathrm{O_2}} \tag{2.2}$$

where $\dot{m}_{\mathrm{in}}$ is the mass flow rate into the compartment (through normal flow in the admission duct or reverse flow in the extraction duct), and $\dot{m}_{\mathrm{out}}$ is the mass flow rate out of the compartment (through normal flow in the extraction duct or reverse flow in the admission duct).

$$\dot{m}_{\mathrm{in}} = \max(0, \dot{m}_{\mathrm{adm}}) + \max(0, -\dot{m}_{\mathrm{ext}}) \tag{2.3}$$

$$\dot{m}_{\mathrm{out}} = \max(0, \dot{m}_{\mathrm{ext}}) + \max(0, -\dot{m}_{\mathrm{adm}}) \tag{2.4}$$

Therefore, combining Equations (2.1) with (2.2), the equation can be written as:

$$m \frac{\mathrm{d}Y_{\mathrm{O_2}}}{\mathrm{d}t} = \dot{m}_{\mathrm{in}} Y_{\mathrm{O_2},\infty} - \dot{m}_{\mathrm{out}} Y_{\mathrm{O_2}} - \dot{\Omega}_{\mathrm{O_2}} - \frac{\mathrm{d}m}{\mathrm{d}t} Y_{\mathrm{O_2}} \tag{2.5}$$

2.1.3 Conservation of mass of fuel

Similarly, the equation for mass of fuel is (there is no fuel coming in from admission):

$$\frac{\mathrm{d}}{\mathrm{d}t} m_{\mathrm{f}} = -\dot{m}_{\mathrm{out}} Y_{\mathrm{f}} + \dot{m}_{\mathrm{f}} - \dot{\Omega}_{\mathrm{f}} \tag{2.6}$$

$$m \frac{\mathrm{d}Y_{\mathrm{f}}}{\mathrm{d}t} = -\dot{m}_{\mathrm{out}} Y_{\mathrm{f}} + \dot{m}_{\mathrm{f}} - \dot{\Omega}_{\mathrm{f}} - \frac{\mathrm{d}m}{\mathrm{d}t} Y_{\mathrm{f}} \tag{2.7}$$

2.1.4 Conservation of energy

The conservation of the internal energy equation is:

$$\frac{\mathrm{d}}{\mathrm{d}t} U = \frac{\mathrm{d}}{\mathrm{d}t} (m C_v T) = \frac{\mathrm{d}}{\mathrm{d}t} (H - PV) \tag{2.8}$$

Combining Equations (2.1) with (2.8), the equation can be written as:

$$\frac{\mathrm{d}}{\mathrm{d}t} U = \dot{m}_{\mathrm{in}} C_p T_\infty - \dot{m}_{\mathrm{out}} C_p T + \dot{Q}_{\mathrm{f}} - \dot{Q}_{\mathrm{loss}} \tag{2.9}$$

Combining Equations (2.8) with (2.9), the equation can be expressed as:

$$m C_v \frac{\mathrm{d}T}{\mathrm{d}t} = \dot{m}_{\mathrm{in}} C_p T_\infty - \dot{m}_{\mathrm{out}} C_p T + \dot{Q}_{\mathrm{f}} - \dot{Q}_{\mathrm{loss}} - \frac{\mathrm{d}m}{\mathrm{d}t} C_v T \tag{2.10}$$

In addition, the heat loss caused by the wall is:

$$\dot{Q}_{\mathrm{loss}} = h A_{\mathrm{w}} (T - T_{\mathrm{w}}) \tag{2.11}$$

where h is the heat exchange coefficient, and A_{w} is the wall area. Here, the temperature T_{w} of the wall is assumed to be constant.

And because of the equation below:

$$m C_v T = \frac{PV}{\gamma - 1} \tag{2.12}$$

Pressure variation can be summarized as:

$$\frac{\mathrm{d}P}{\mathrm{d}t} = \frac{\gamma - 1}{V}(\dot{m}_{\mathrm{in}} C_p T_\infty - \dot{m}_{\mathrm{out}} C_p T + \dot{Q}_{\mathrm{f}} - \dot{Q}_{\mathrm{loss}}) \tag{2.13}$$

2.2 Combustion regime

The combustion in the model is governed by its regimes. The ratio of oxygen and fuel consumed during the combustion reaction influences the mass loss rate and the heat release rate.

2.2.1 Global equivalence ratio

The ratio of oxygen and fuel plays an important role during this research, and hence, a detailed study on this is required. Generally, the global equivalence ratio (GER) study is performed in a steady state; however, the variation of GER along with the time is preferred in this study. Therefore, a variable rs is introduced, which means the oxygen-to-fuel mass ratio:

$$rs = \frac{m_{\mathrm{O}_2}}{m_f} \tag{2.14}$$

Z represents mixture fraction:

$$Z = \frac{rsY_{\mathrm{f}} - Y_{\mathrm{O}_2} + Y_{\mathrm{O}_2,\infty}}{rs + Y_{\mathrm{O}_2,\infty}} \tag{2.15}$$

For the situation of a stoichiometric status:

$$Z_{\mathrm{st}} = \frac{Y_{\mathrm{O}_2,\infty}}{rs + Y_{\mathrm{O}_2,\infty}} \tag{2.16}$$

Therefore, the compartment global equivalence ratio ϕ is described as:

$$\phi = rs\frac{m_{\mathrm{f}}}{m_{\mathrm{O_2}}} = \frac{Z(1-Z_{\mathrm{st}})}{Z_{\mathrm{st}}(1-Z)} \tag{2.17}$$

2.2.2 Over-ventilation

When $\phi < 1$, the ventilation regime is named over-ventilation, where there is enough oxygen but limited fuel. Therefore, the fuel consumed during this reaction is equal to its mass loss because all the fuel is consumed:

$$\dot{\Omega}_{\mathrm{f}} = \dot{m}_{\mathrm{f}} \tag{2.18}$$

The stoichiometric status can be applied here, hence, the amount of oxygen is:

$$\dot{\Omega}_{\mathrm{O_2}} = rs \times \dot{\Omega}_{\mathrm{f}} \tag{2.19}$$

The rate of heat released by the combustion is:

$$\dot{Q}_{\mathrm{f}} = \Delta H_{\mathrm{f}} \times \dot{\Omega}_{\mathrm{f}} \tag{2.20}$$

where ΔH_{f} is the heat of combustion (per unit mass of fuel).

2.2.3 Under-ventilation

When $\phi > 1$, the ventilation regime is named under-ventilation, where there is plenty of fuel but limited oxygen. Therefore, the fuel consumed during this reaction depends on the amount of oxygen:

$$\dot{\Omega}_{\mathrm{O_2}} = \dot{m}_{\mathrm{in}} Y_{\mathrm{O_2},\infty} \tag{2.21}$$

$$\dot{\Omega}_{\mathrm{f}} = \frac{\dot{\Omega}_{\mathrm{O_2}}}{rs} \tag{2.22}$$

The rate of heat released by the combustion is:

$$\dot{Q}_{\mathrm{f}} = \Delta H_{\mathrm{f}} \times \dot{\Omega}_{\mathrm{f}} \tag{2.23}$$

In the simulation, a ϕ-based weigh coefficient F is introduced to help to obtain a continuous transition between these two combustion regimes:

$$F = 0.5 - 0.5\tanh(\frac{\phi\text{-}1}{0.025}) \tag{2.24}$$

$$\dot{\Omega}_F = \dot{m}_f F + (1-F)\frac{\dot{m}_{in} Y_{O_2,\infty}}{rs} \tag{2.25}$$

$$\dot{\Omega}_{O_2} = \dot{\Omega}_f \times rs \tag{2.26}$$

$$\dot{Q}_f = \dot{\Omega}_f \times \Delta H_f \tag{2.27}$$

However, the Equations (2.24) ~ (2.27) are only suitable to the flame without extinction, therefore the equations for the extinction model are developed as:

$$FEF = 0.5 + 0.5\tanh(\frac{Y_{O_2}\text{-}Y_{O_2,critical}}{0.01}) \tag{2.28}$$

$$\dot{\Omega}_f^* = \dot{\Omega}_f \times FEF \tag{2.29}$$

$$\dot{\Omega}_{O_2}^* = \dot{\Omega}_f^* \times rs \tag{2.30}$$

$$\dot{Q}_f^* = \dot{\Omega}_f^* \times \Delta H_f \tag{2.31}$$

2.3 Airflow through compartment

In a fire scenario, the pressure difference between the compartment and the outdoor environment is complex, therefore, two more equations which describe the mechanical flow of admission and extraction are considered to be added in.

Bernoulli's model, which helps associate the ventilation with pressure, is considered here as a basis (it is mainly used to solve steady states problems). Therefore, for the admission duct, the equation can be developed as:

$$\frac{L_{\text{adm}}}{S_{\text{adm}}}\frac{\mathrm{d}\dot{m}_{\text{adm}}}{\mathrm{d}t} = P_{\text{adm}} - P - \varepsilon_{\text{adm}} r_{\text{adm}} \frac{\dot{m}_{\text{adm}}^2}{\rho_{\text{adm}}} \tag{2.32}$$

where L_{adm} is the length of the admission duct, S_{adm} is the surface area of the section of the admission duct, and r_{adm} usually comes from experimental measurement which equals to $\frac{1}{2(C_d)^2(S_{\text{adm}})^2}$, and $C_d \approx 0.6 \sim 0.7$.

For the extraction duct, the equation can be written as:

$$\frac{L_{\text{ext}}}{S_{\text{ext}}}\frac{\mathrm{d}\dot{m}_{\text{ext}}}{\mathrm{d}t} = P - P_{\text{ext}} - \varepsilon_{\text{ext}} r_{\text{ext}} \frac{\dot{m}_{\text{ext}}^2}{\rho_{\text{ext}}} \tag{2.33}$$

For these two equations, the determination of the flow direction needs to be noticed:

When $\dot{m}_{\text{adm}} \geq 0$, $\varepsilon_{\text{adm}} = 1$; otherwise, $\varepsilon_{\text{adm}} = -1$; similarly, when $\dot{m}_{\text{ext}} \geq 0$, $\varepsilon_{\text{ext}} = 1$, otherwise, $\varepsilon_{\text{ext}} = -1$

2.4 Synthesis

This form summarizes all the equations used in the numerical model for this study on compartment fires:

Table 2-1 Summary of equations used in the model

Unknown	**Equation**	**ODE**
$\dot{m}(t)$	$\frac{\mathrm{d}m}{\mathrm{d}t} = \dot{m}_{\mathrm{adm}} - \dot{m}_{\mathrm{ext}} + \dot{m}_{\mathrm{f}}$	x(2)
$\dot{m}_{\mathrm{adm}}(t)$	$\frac{L_{\mathrm{adm}}}{S_{\mathrm{adm}}}\frac{\mathrm{d}\dot{m}_{\mathrm{adm}}}{\mathrm{d}t} = P_{\mathrm{adm}} - P - \varepsilon_{\mathrm{adm}} r_{\mathrm{adm}} \frac{\dot{m}_{\mathrm{adm}}^2}{\rho_{\mathrm{adm}}}$	x(4)
$\dot{m}_{\mathrm{ext}}(t)$	$\frac{L_{\mathrm{ext}}}{S_{\mathrm{ext}}}\frac{\mathrm{d}\dot{m}_{\mathrm{ext}}}{\mathrm{d}t} = P - P_{\mathrm{ext}} - \varepsilon_{\mathrm{ext}} r_{\mathrm{ext}} \frac{\dot{m}_{\mathrm{ext}}^2}{\rho_{\mathrm{ext}}}$	x(5)
$Y_{\mathrm{O_2}}(t)$	$m\frac{\mathrm{d}Y_{\mathrm{O_2}}}{\mathrm{d}t} = \dot{m}_{\mathrm{in}} Y_{\mathrm{O_2},\infty} - \dot{m}_{\mathrm{out}} Y_{\mathrm{O_2}} - \dot{\Omega}_{\mathrm{O_2}} - \frac{\mathrm{d}m}{\mathrm{d}t} Y_{\mathrm{O_2}}$	x(6)
$Y_{\mathrm{f}}(t)$	$m\frac{\mathrm{d}Y_{\mathrm{f}}}{\mathrm{d}t} = -\dot{m}_{\mathrm{out}} Y_{\mathrm{f}} + \dot{m}_{\mathrm{f}} - \dot{\Omega}_{\mathrm{f}} - \frac{\mathrm{d}m}{\mathrm{d}t} Y_{\mathrm{f}}$	x(7)
$T(t)$	$mC_v\frac{\mathrm{d}T}{\mathrm{d}t} = \dot{m}_{\mathrm{in}} C_p T_\infty - \dot{m}_{\mathrm{out}} C_p T + \dot{Q}_{\mathrm{f}} - \dot{Q}_{\mathrm{loss}} - \frac{\mathrm{d}m}{\mathrm{d}t} C_v T$	x(3)
$P(t)$	$\frac{\mathrm{d}P}{\mathrm{d}t} = \frac{\gamma - 1}{V}(\dot{m}_{\mathrm{in}} C_p T_\infty - \dot{m}_{\mathrm{out}} C_p T + \dot{Q}_{\mathrm{f}} - \dot{Q}_{\mathrm{loss}})$	x(1)

Relation 1 (equivalence ratio)
$Z = \frac{rsY_{\mathrm{f}} - Y_{\mathrm{O_2}} + Y_{\mathrm{O_2,air}}}{rs + Y_{\mathrm{O_2,air}}}$
$Z_{\mathrm{st}} = \frac{Y_{\mathrm{O_2,air}}}{rs + Y_{\mathrm{O_2,air}}}$
$\phi = rs\frac{m_{\mathrm{f}}}{m_{\mathrm{O_2}}} = \frac{Z(1-Z_{\mathrm{st}})}{Z_{\mathrm{st}}(1-Z)}$

Relation 2.1 (flame model without extinction)
$F = 0.5 - 0.5\tanh\left(\frac{\phi\text{-}1}{0.025}\right)$
$\dot{\Omega}_{\mathrm{F}} = \dot{m}_{\mathrm{f}} F + (1-F)\frac{\dot{m}_{\mathrm{in}} Y_{\mathrm{O_2,air}}}{rs}$
$\dot{\Omega}_{\mathrm{O_2}} = \dot{\Omega}_{\mathrm{f}} \times rs$
$\dot{Q}_{\mathrm{f}} = \dot{\Omega}_{\mathrm{f}} \times \Delta H_{\mathrm{f}}$

Relation 2.2 (flame model with extinction)
$FEF = 0.5 + 0.5\tanh\left(\frac{Y_{O_2} - Y_{O_2,\text{critical}}}{0.01}\right)$
$\dot{\Omega}_f^* = \dot{\Omega}_f \times FEF$
$\dot{\Omega}_{O_2}^* = \dot{\Omega}_f^* \times rs$
$\dot{Q}_f^* = \dot{\Omega}_f^* \times \Delta H_f$

3 Verification tests

This chapter is to apply the verification tests to the preliminary model. Three verifications are performed in this chapter: the first one is to test the convergence of the environment parameters, and then use the hand calculation (in steady state) derived by Bernoulli's method to verify the model. The second one is to use a designed mass loss rate to simulate three ventilation regimes, in addition, Burke-Schuman formula is used here to verify the model. The third one is to test the oscillatory behavior by using Helmholtz oscillation theory.

3.1 Pressure-flow coupling without fire

In this model, Equations (2.32) and (2.33) are used to describe mass flow rates (inflow and outflow). Meanwhile, Bernoulli's model can be used to calculate the values of air blown in and out in a steady state by hand:

$$\dot{m}_{\text{adm}} = \text{sign}(P_{\text{adm}} - P)\left(\frac{\rho_{\text{adm}}(P_{\text{adm}} - P)}{r_{\text{adm}}}\right)^{\frac{1}{2}} \tag{3.1}$$

$$\dot{m}_{\text{ext}} = \text{sign}(P - P_{\text{ext}})\left(\frac{\rho(P - P_{\text{ext}})}{r_{\text{ext}}}\right)^{\frac{1}{2}} \tag{3.2}$$

Furthermore, since there is no fire in this test, Equations (2.10) and (2.13) can be simplified as:

$$mC_v\frac{\mathrm{d}T}{\mathrm{d}t} = \dot{m}_{\text{in}}C_pT_\infty - \dot{m}_{\text{out}}C_pT - \dot{Q}_{\text{loss}} \tag{3.3}$$

$$\frac{\mathrm{d}P}{\mathrm{d}t} = \frac{\gamma - 1}{V}\left(\dot{m}_{\text{in}}C_pT_\infty - \dot{m}_{\text{out}}C_pT - \dot{Q}_{\text{loss}}\right) \tag{3.4}$$

It is noted that P is an unknown variable and mainly depends on the blowing speed and resistance loss. Therefore, different values of P can be used to check the stability of the model.

The initial conditions for the input parameters are listed as below:

$r_{\text{adm}} = 420\ (\text{m}^{-4}),\ r_{\text{ext}} = 2886\ (\text{m}^{-4})$

$P_0 = 101325\ (\text{Pa})$

$P_{\text{adm}}(t_0) = P_0 + 126\ (\text{Pa}),\ P_{\text{ext}}(t_0) = P_0 - 866\ (\text{Pa})$

$\text{T}(t_0) = 293\ (\text{K})$

$C_p = 1000\ (\text{J/kg}\cdot\text{K})$

$P_1 = (P_0 - 966)\ (\text{Pa}),\ P_2 = P_0,\ P_3 = (P_0 + 226)\ (\text{Pa})$

$\dot{m}_{\text{adm}}(t_0) = \dot{m}_{\text{ext}}(t_0) = 0\ (\text{kg/s})$

These figures are plotted as below:

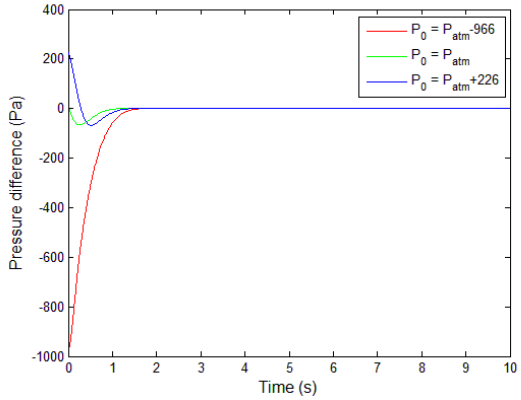

Figure 3-1 Time variation of pressure difference, a verification test of pressure-flow coupling with fire (t=10 s)

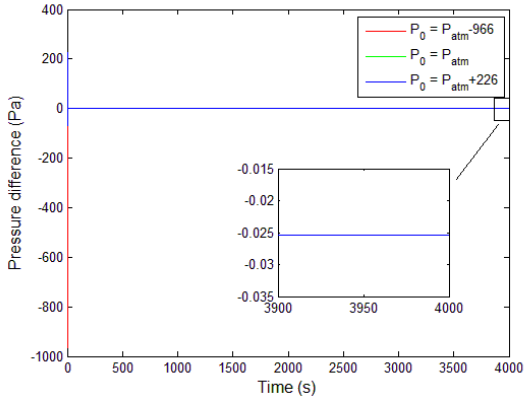

Figure 3-2 Time variation of pressure difference, a verification test of pressure-flow coupling with fire (t=4000 s)

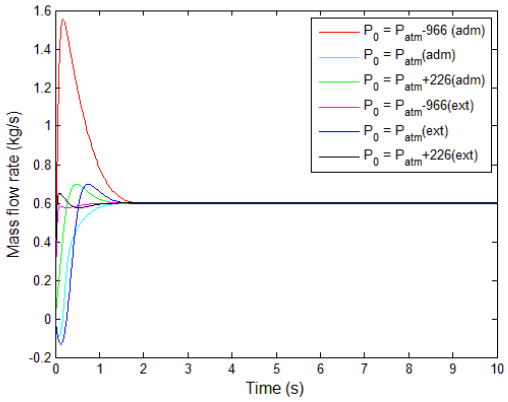

Figure 3-3 Time variation of mass flow rate, a verification test of pressure-flow coupling with fire (t=10 s)

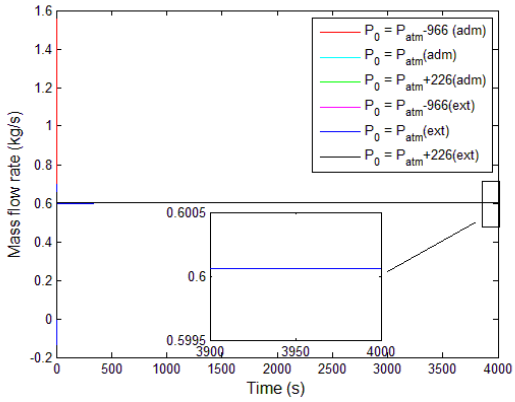

Figure 3-4 Time variation of mass flow rate, a verification test of pressure-flow coupling with fire (t=4000 s)

Though the input P is a variable, the simulation results of pressure and mass flow rate all show a convergence to a stable system after some time.

Moreover, Equation (3.1) and (3.2) are used for hand-calculating the pressure difference value during stable state to check the model:

$$\dot{m}_{\text{adm}} \approx \dot{m}_{\text{ext}} \approx 0.6000 \text{ (kg/s)} \Rightarrow \left(\frac{\rho_{\text{adm}} (P_{\text{adm}} - P)}{r_{\text{adm}}} \right)^{\frac{1}{2}} = \left(\frac{\rho_{\text{ext}} (P - P_{\text{ext}})}{r_{\text{ext}}} \right)^{\frac{1}{2}} \quad (3.5)$$

$$\Delta P = P - P_0 = \frac{\dfrac{\rho_{\text{adm}} P_{\text{adm}}}{r_{\text{adm}}} + \dfrac{\rho_{\text{ext}} P_{\text{ext}}}{r_{\text{ext}}}}{\dfrac{\rho_{\text{adm}}}{r_{\text{adm}}} + \dfrac{\rho_{\text{ext}}}{r_{\text{ext}}}} - P_0 \approx -0.0255 \text{ Pa} \quad (3.6)$$

It is noted that the result of the hand calculated P equals to -0.025 Pa marked in Figure 3-2 (in steady state); so is the situation of $\dot{m}_{\text{adm}}$ and $\dot{m}_{\text{ext}}$, where input value 0.6 kg/s is closed to 0.6001 kg/s that marked in Figure 3-4 . Therefore, this model is quantitatively correct.

3.2 Preliminary tests by using a designed mass loss rate

Equations (2.32) and (2.33) are also used in this section.

3.2.1 Over-ventilation regime ($\phi < 1$)

In this case, enough oxygen is blown into the compartment; that is to say, there is enough oxygen to consume the fuel.

Mass loss rate is designed and described as:

$$\dot{m}_{\mathrm{f}} = \min(\alpha t^2, 0.01) \text{ (kg/s)} \tag{3.7}$$

It is noticeable that heptane is selected as the fuel, and therefore, its value of stoichiometric oxygen-to-fuel mass ratio is calculated as:

$$rs = \frac{m_{\mathrm{O_2}}}{m_{\mathrm{f}}} = \frac{M_{\mathrm{O_2}} n_{\mathrm{O_2}}}{M_{\mathrm{f}} n_{\mathrm{f}}} = \frac{16 \text{ g/mol} \times 2 \times 11}{12 \text{ g/mol} \times 7 + 1 \text{ g/mol} \times 16} \approx 3.52 \tag{3.8}$$

The corresponding global equivalence ratio-based weigh coefficient is described by using Equation (2.17) above.

The initial conditions for the input parameters are listed as below:

$r_{\mathrm{adm}} = 420$ (m^{-4}), $r_{\mathrm{ext}} = 2886$ (m^{-4})
$P_0 = 101325$ (Pa)
$P_{\mathrm{adm}}(t_0) = P_0 + 172$ (Pa), $P_{\mathrm{ext}}(t_0) = P_0 - 1178$ (Pa)
$\mathrm{T}(t_0) = 293$ (K), $T_{\mathrm{w}}(t_0) = 293$ (K)
$\Delta \mathrm{H}_{\mathrm{f}} = 44.56$ (MJ/kg)
$\alpha = 10^{-7}$ ($\mathrm{kg/s}^3$)
$\dot{m}_{\mathrm{adm}}(t_0) = \dot{m}_{\mathrm{ext}}(t_0) = 0.696521$ (kg/s)

where $\dot{m}_{\mathrm{adm}} = \dot{m}_{\mathrm{ext}}$ are calculated at steady state without a fire. In the code, a function file which describes this no fire situation is used to derive the initial values for the reaction.

The output figures are shown as below:

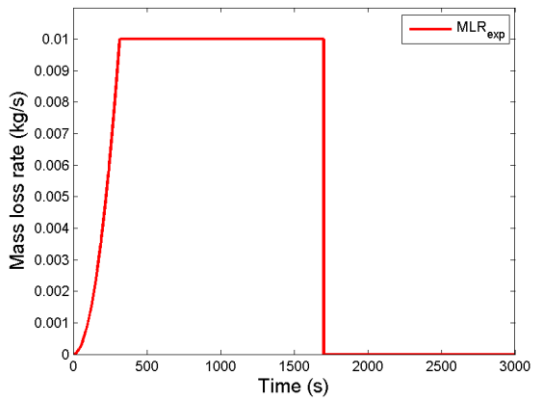

Figure 3-5 Time variation of mass loss rate, a preliminary test by using a designed mass loss rate in the over-ventilation regime

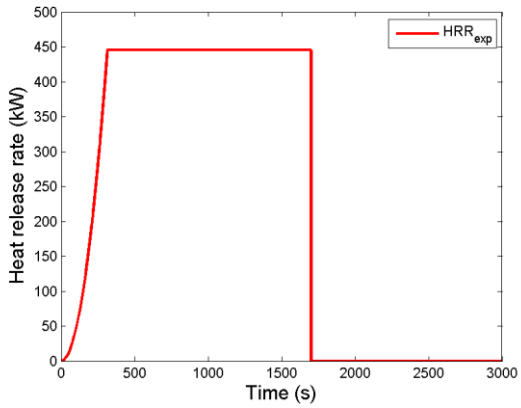

Figure 3-6 Time variation of heat release rate, a preliminary test by using a designed mass loss rate in the over-ventilation regime

Figure 3-5 is the time variation of a designed fuel mass loss rate of the fuel source (heptane). The curve first increases as second order power function before 300 s; after that, it maintains steady; it ultimately drops to 0 immediately as the fuel source is depleted at 1700 s.

Similarly, Figure 3-6 describes the variation of heat release rate versus time; it has similar the tendency as it does in Figure 3-5 and Figure 3-7. All of them first increase to a stable state, and then to extinct.

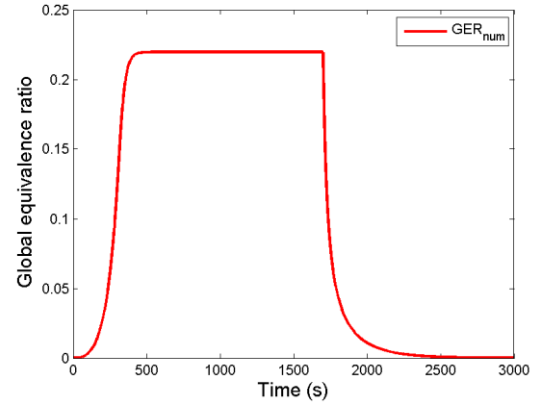

Figure 3-7 Time variation of global equivalence ratio, a preliminary test by using a designed mass loss rate in the over-ventilation regime

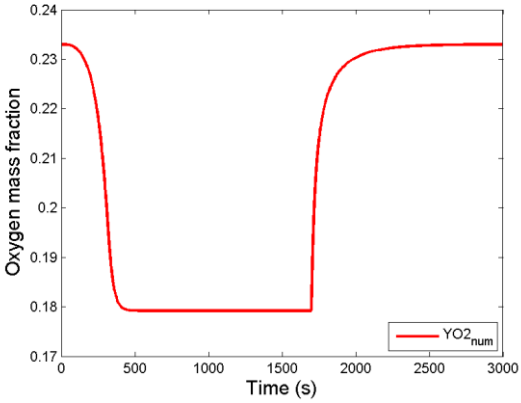

Figure 3-8 Time variation of oxygen mass fraction, a preliminary test by using a designed mass loss rate in the over-ventilation regime

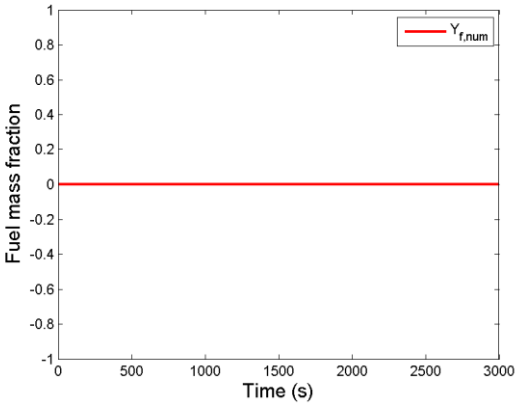

Figure 3-9 Time variation of fuel mass fraction, a preliminary test by using a designed mass loss rate in the over-ventilation regime

Figure 3-7 shows the time variation of global equivalence ratio, which shares a similar tendency with Figure 3-5 and 3-6; the maximum value (in the steady state) in Figure 3-7 is about 0.22.

Figure 3-8 shows the variation of oxygen mass fraction along with the time, and its minimum value (in the steady state) is closed to 0.18. Therefore, Burke-Schuman formula can be used here to check the value of oxygen mass fraction in the steady state:

$$Y_{O_2} = \frac{Y_{O_2,\infty}(1-\phi)}{1+\frac{\phi Y_{O_2,\infty}}{rs}} \tag{3.9}$$

where $Y_{O_2,\infty} \approx 23.3\%$ is the input oxygen mass fraction in the ambient air. The calculated Y_{O_2} is about 0.18, which corresponds to the value in the Figure 3-8.

Figure 3-9 shows the variation of fuel mass fraction along with the time. It remains 0 since the regime in this case is over-ventilation, which means enough oxygen can be provided to consume all the fuel.

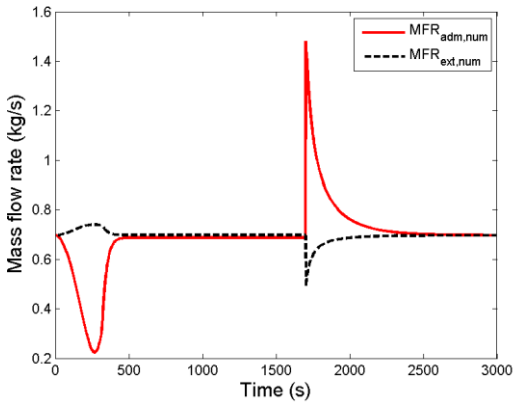

Figure 3-10 Time variation of mass flow rate, a preliminary test by using a designed mass loss rate in the over-ventilation regime

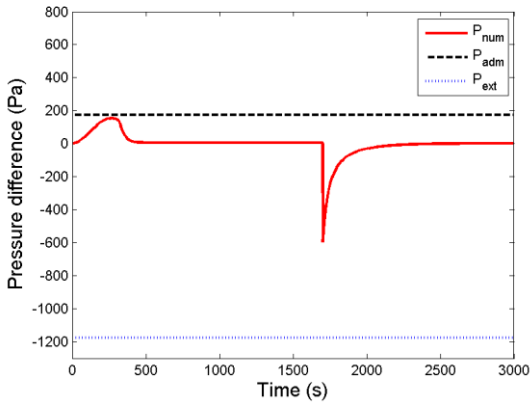

Figure 3-11 Time variation of pressure difference, a preliminary test by using a designed mass loss rate in the over-ventilation regime

In Figure 3-10, both plots of admission and extraction mass flow rates fluctuate during the transition state. Moreover, during the steady state, both plots remain stable. After the extinction, two curves come to a same value. There is no reverse flow in this case according to Figure 3-10 and 3-11.

3.2.2 Under-ventilation regime (ϕ >1, without flame extinction)

In this case, there is not enough oxygen blown into the compartment, and therefore, flame extinction may exist. To begin with, a model without flame extinction is applied for preliminary test.

The global equivalence ratio-based weigh coefficient used here is described in Equation (2.24) as above. Meanwhile, input $\dot{m}_f$ and rs remain the same. Other initial conditions for the input parameters are listed here:

$r_{adm} = 42122\ (\mathrm{m}^{-4}),\ r_{ext} = 288490\ (\mathrm{m}^{-4})$

$P_0 = 101325$ (Pa)

$P_{adm}(t_0) = P_0 + 172$ (Pa), $P_{ext}(t_0) = P_0 - 1178$ (Pa)

$\mathrm{T}(t_0) = 293$ (K), $T_w(t_0) = 293$ (K)

$\Delta \mathrm{H}_f = 44.56$ (MJ/kg)

$\alpha = 10^{-7}\ (\mathrm{kg/s}^3)$

$\dot{m}_{adm}(t_0) = \dot{m}_{ext}(t_0) = 0.069651$ (kg/s)

where $\dot{m}_{adm} = \dot{m}_{ext}$ are calculated at steady state without a fire as above. In the code, a function file which describes the no fire situation is used to derive the initial mass flow rates.

The figures are listed as below:

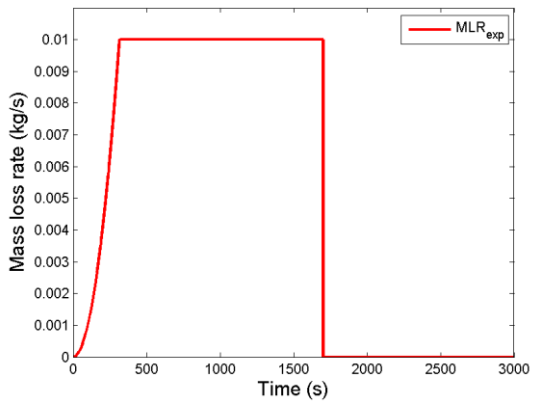

Figure 3-12 Time variation of mass loss rate, a preliminary test by using a designed mass loss rate in the under-ventilation regime without extinction

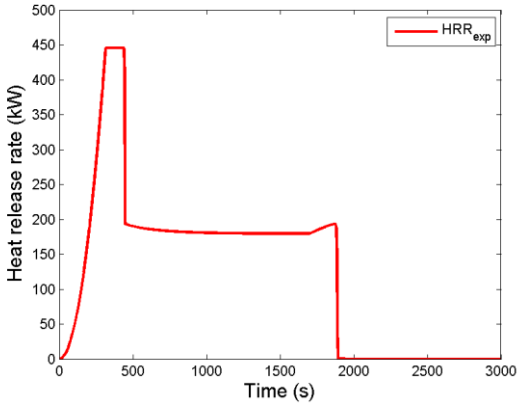

Figure 3-13 Time variation of heat release rate, a preliminary test by using a designed mass loss rate in the under-ventilation regime without extinction

Figure 3-12 is the time variation of a designed fuel mass loss rate, which is the same as the curve used in the over-ventilation regime test.

Figure 3-13 describes the heat release rate change along with the time; it decreases after the system switching to the under-ventilated regime (without enough oxygen) at about 450 s, though the fuel mass flow is imposed constantly.

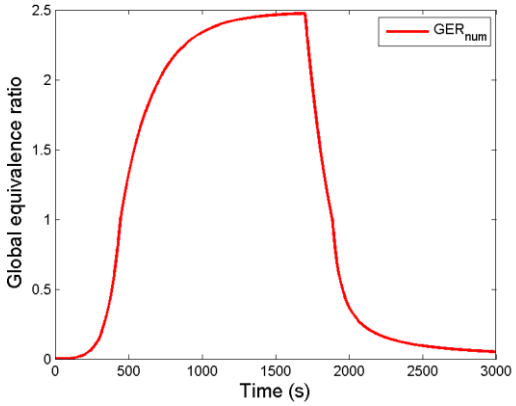

Figure 3-14 Time variation of global equivalence ratio, a preliminary test by using a designed mass loss rate in the under-ventilation regime without extinction

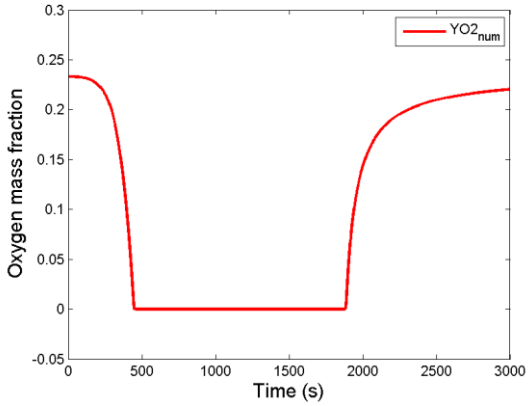

Figure 3-15 Time variation of oxygen mass fraction, a preliminary test by using a designed mass loss rate in the under-ventilation regime without extinction

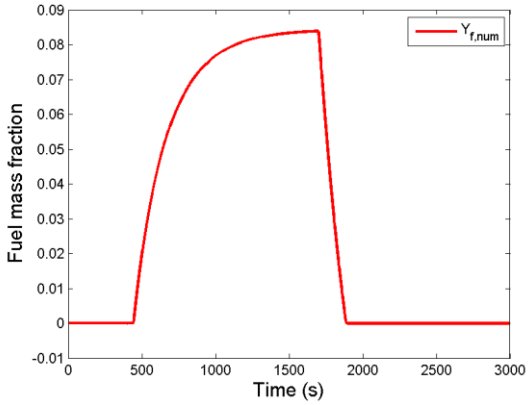

Figure 3-16 Time variation of fuel mass fraction, a preliminary test by using a designed mass loss rate in the under-ventilation regime without extinction

In Figure 3-14, the curve first keeps increasing because oxygen is over-consumed (without extinction), but the rate fuel input remains consistent. After the exhaustion of the fuel, the curve drops gradually due to the continued oxygen inflow.

In Figure 3-15, at about 450 s, the oxygen mass fraction drops to 0 due to its low supply rate, and the situation is not changed before the fuel being used up. To note, small negative values may be derived during the simulation. However, in reality, the combustion cannot be maintained when the value of oxygen mass fraction is at

this low level; therefore, a more explicit model (with extinction) should be considered in the following verification in the next chapter.

In Figure 3-16, the fuel mass fraction first remains 0 as there is enough oxygen to ensure fully combustion; after that, it keeps increasing until the fuel is used up; finally, it drops to 0 again due to the fuel depletion and inflow oxygen.

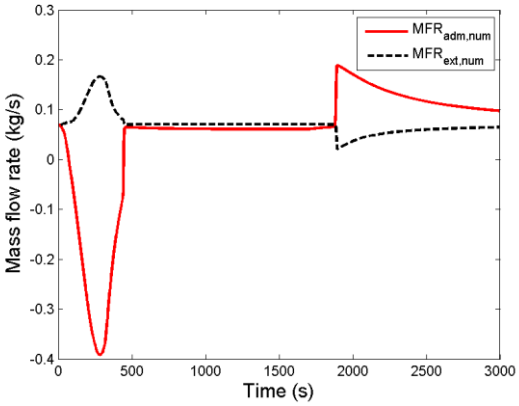

Figure 3-17 Time variation of mass flow rate, a preliminary test by using a designed mass loss rate in the under-ventilation regime without extinction

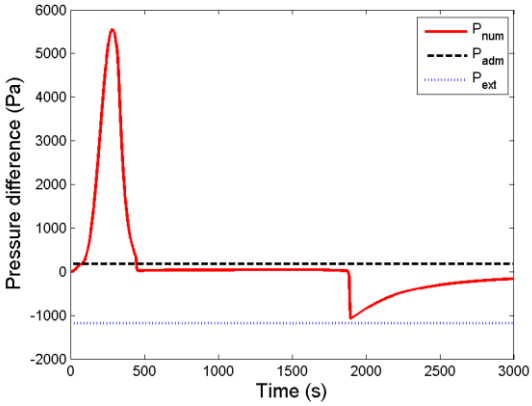

Figure 3-18 Time variation of pressure difference, a preliminary test by using a designed mass loss rate in the under-ventilation regime without extinction

According to these two figures, a reversal admission flow phenomenon can be observed. An overpressure phenomenon appears during the start time of combustion as it is shown in Figure 3-18. Correspondingly, the admission duct is used for outflow as it is indicated in Figure 3-17. There is no reverse flow during extinction period in this case. Ultimately, the system returns to a steady state after the disturbance.

3.2.3 Under-ventilation regime ($\phi > 1$, with flame extinction)

In this case, a model with flame extinction is used to compare with the one without extinction in section 3.2.2. This model should be more reasonable because not only the amount of fuel source is the precondition of the combustion, but also

consider the influence of concentration of oxygen, temperature and so on. Therefore, a more precise model is required to simulate the combustion.

Input parameters remain the same as they are shown above.

The global equivalence ratio-based weigh coefficient FEF=0.12 (see Equation (2.28)) is used here to describe the model with flame extinction. The value of 0.12 is used in this case and its selection will be discussed in the next chapter.

These figures are plotted as below:

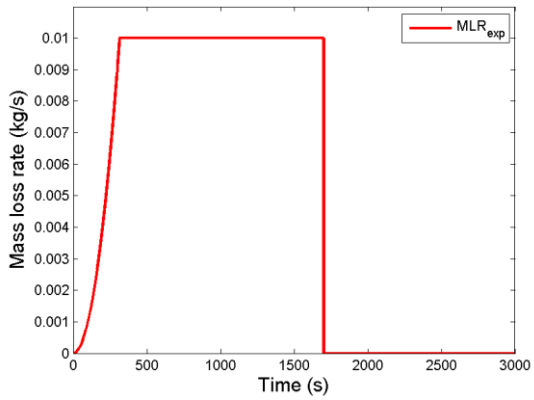

Figure 3-19 Time variation of mass loss rate, a preliminary test by using a designed mass loss rate in the under-ventilation regime with extinction

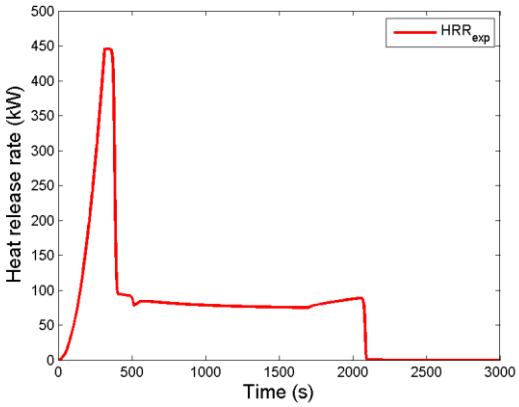

Figure 3-20 Time variation of heat release rate, a preliminary test by using a designed mass loss rate in the under-ventilation regime with extinction

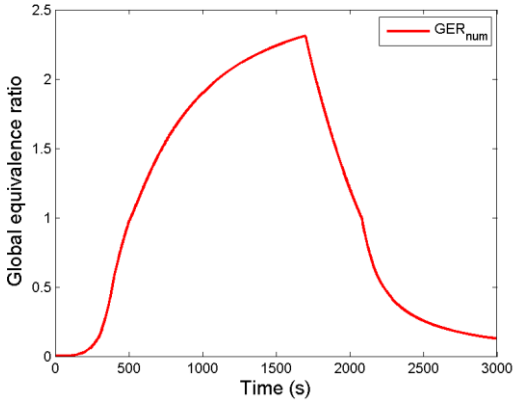

Figure 3-21 Time variation of global equivalence ratio, a preliminary test by using a designed mass loss rate in the under-ventilation regime with extinction

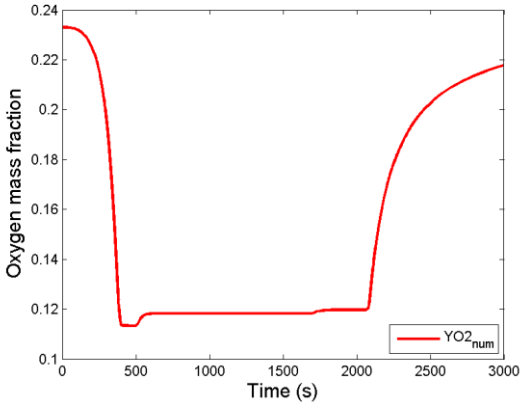

Figure 3-22 Time variation of oxygen mass fraction, a preliminary test by using a designed mass loss rate in the under-ventilation regime with extinction

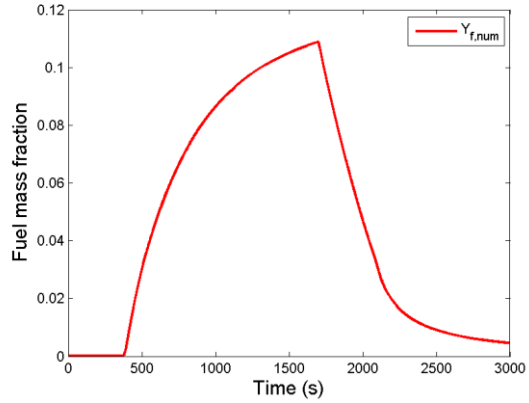

Figure 3-23 Time variation of fuel mass fraction, a preliminary test by using a designed mass loss rate in the under-ventilation regime with extinction

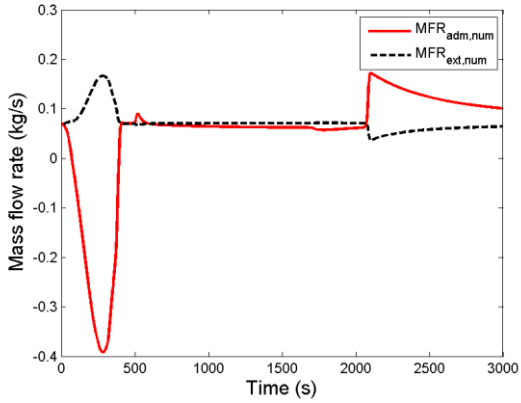

Figure 3-24 Time variation of mass flow rate, a preliminary test by using a designed mass loss rate in the under-ventilation regime with extinction

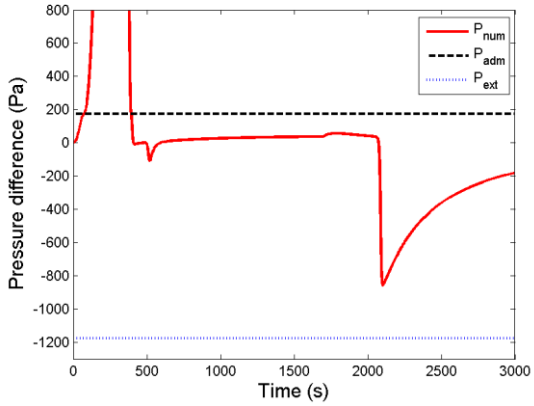

Figure 3-25 Time variation of pressure difference, a preliminary test by using a designed mass loss rate in the under-ventilation regime with extinction

These figures are plotted from the model containing flame extinction; therefore, the curves in Figure 3-20 – Figure 3-25 are different from the corresponding ones in Figure 3-13-3.18, even though they share the same input parameters.

For example , the maximum value of heat release rate in Figure 3-20 does not decrease before the value of global equivalence ratio in Figure 3-21 is larger than 1. After that, the extinction model has effects on the results, for example, the maximum

value of global equivalence ratio in Figure 3-21 is smaller than that in Figure 3-14; the minimum value in Figure 3-22 which describes the oxygen mass fraction is larger than that in Figure 3-15; and the maximum value in Figure 3-23 which describes the fuel mass fraction is larger than that in Figure 3-16, since there is no combustion when oxygen mass fraction is less than 0.12 (which reflects the actual flame scenarios). In addition, the time spent to achieve a steady state is extended. However, the ultimate values of mass flow rate and pressure are close in different models, regardless of there is extinction or not.

3.3 Preliminary tests by using Helmholtz oscillation theory

3.3.1 Calculations for the frequency

In this part, Equations (2.13), (2.32) and (2.33) are used to hand-calculate the frequency:

$$\frac{\mathrm{d}^2 P}{\mathrm{d}t^2} = \varepsilon \frac{\gamma - 1}{V} C_p T_\infty \left(\frac{\mathrm{d}\dot{m}_{\mathrm{adm}}}{\mathrm{d}t} - \frac{\mathrm{d}\dot{m}_{\mathrm{ext}}}{\mathrm{d}t} \right) \tag{3.10}$$

where ε is used to control the switch of inflow and outflow scenarios. There is no fire or wall loss in this case.

Equations (2.32) and (2.33) are used to replace the corresponding items in Equation (3.10):

$$\begin{aligned}
\frac{\mathrm{d}^2 P}{\mathrm{d}t^2} &= \varepsilon \frac{\gamma - 1}{V} C_p T_\infty \left[\frac{S_{\mathrm{adm}}}{L_{\mathrm{adm}}} \left(P_{\mathrm{adm}} - P - \varepsilon_{\mathrm{adm}} r_{\mathrm{adm}} \frac{\dot{m}_{\mathrm{adm}}^2}{\rho_{\mathrm{adm}}} \right) - \frac{S_{\mathrm{ext}}}{L_{\mathrm{ext}}} \left(P - P_{\mathrm{ext}} - \varepsilon_{\mathrm{ext}} r_{\mathrm{ext}} \frac{\dot{m}_{\mathrm{ext}}^2}{\rho_{\mathrm{ext}}} \right) \right] \\
&= \varepsilon \frac{\gamma - 1}{V} C_p T_\infty \frac{S}{L} \left[\left(P_{\mathrm{adm}} - P \right) - \left(P - P_{\mathrm{ext}} \right) \right] \\
&= \varepsilon \frac{\gamma - 1}{V} C_p T_\infty \frac{S}{L} \left[P_{\mathrm{adm}} - 2P + P_{\mathrm{ext}} \right]
\end{aligned}$$

(3.11)

where $S_{\text{adm}} = S_{\text{ext}} = S$, $L_{\text{adm}} = L_{\text{ext}} = L$; meanwhile, damping items are neglected here.

Moreover, in the Helmholtz system:

$$\omega_0 = \sqrt{\frac{2S}{L} C_p T_\infty \frac{\gamma - 1}{V}} \approx 5.9562 \text{ (rad/s)} \tag{3.12}$$

$$T_0 = \frac{2\pi}{\omega_0} \approx 1.0544 \text{ (s)} \tag{3.13}$$

where T_0 is the period of the pressure signal.

Therefore, Equation (3.11) can be re-written as:

$$\frac{\mathrm{d}^2 P}{\mathrm{d}t^2} + \omega_0^2 P = \frac{\omega_0^2}{2}\left(P_{\text{adm}} + P_{\text{ext}}\right) \tag{3.14}$$

3.3.2 A simulation with a constant temperature

This test describes a simulation with a constant temperature to explore the unstable behaviors.

The initial conditions are listed as below:

$r_{\text{adm}} = 0$ (m^{-4}), $r_{\text{ext}} = 0$ (m^{-4})
$P_0 = 101325$ (Pa)
$P_{\text{adm}}(t_0) = P_0 + 500$ (Pa), $P_{\text{ext}}(t_0) = P_0 - 300$ (Pa)
$\dot{m}_{\text{adm}} = \dot{m}_{\text{ext}} = 0$ (kg/s)
$T(t_0) = 293$ (K)
$L = 10$ (m), $S = 0.18$ (m^2), $V = 120$ (m^3)
$\gamma = 1.4$

The pressure difference plot is shown below:

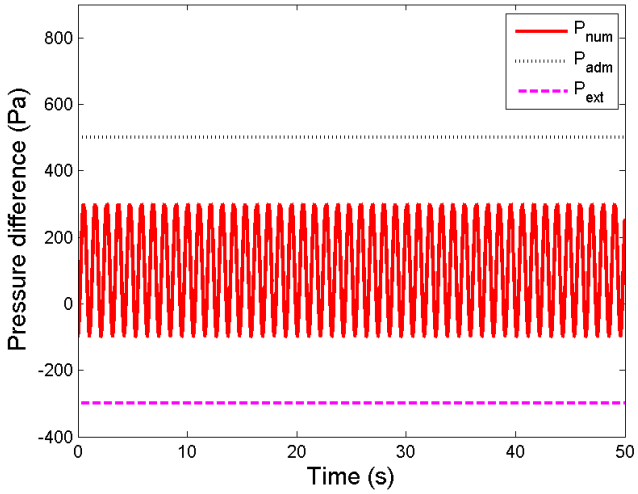

Figure 3-26 Time variation of pressure difference, a preliminary tests by using Helmholtz oscillation theory (with a constant pressure)

A periodic oscillation, which was plotted at a constant temperature situation with no fire, can be observed in Figure 3-26. The curve oscillations are uniform with constant extreme values and period. According to the plot, the result of the period is approximately 1, which is close to the value of T_0 by the hand-calculation in the previous section above.

3.3.3 A simulation with a variable temperature

This test describes a simulation with a variable temperature to explore the unstable behaviors.

The initial conditions for the input parameters are listed here:

$r_{\text{adm}} = 0\ (\text{m}^{-4}),\ r_{\text{ext}} = 0\ (\text{m}^{-4})$
$P_0 = 101325\ (\text{Pa}),\ P(t_0) = P_0 + 30\ (\text{Pa})$
$P_{\text{adm}}(t_0) = P_0 + 500\ (\text{Pa}),\ P_{\text{ext}}(t_0) = P_0 - 300\ (\text{Pa})$
$\dot{m}_{\text{adm}} = \dot{m}_{\text{ext}} = 0\ (\text{kg/s})$
$T(t_0) = 293\ (\text{K}),\ T_{\text{adm}} = \text{T}(t_0)\ (\text{K})$
$L = 10\ (\text{m}),\ S = 0.18\ (\text{m}^2),\ V = 120\ (\text{m}^3)$
$\gamma = 1.4$

The pressure difference and temperature plots are listed below:

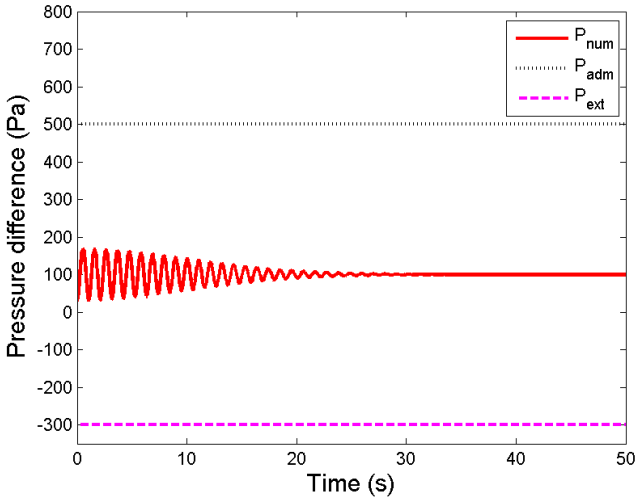

Figure 3-27 Time variation of pressure difference, a preliminary tests by using Helmholtz oscillation theory (with a variable pressure)

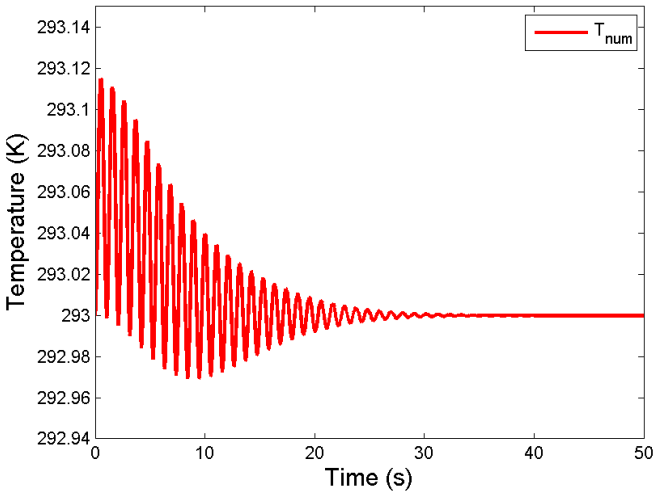

Figure 3-28 Time variation of temperature, a preliminary tests by using Helmholtz oscillation theory (with a variable pressure)

A periodic oscillation, which was plotted at a variable temperature situation with no fire, can also be observed in both Figure 3-27 and 3-28. The amplitudes of the curves are no more uniform and the oscillations ultimately turn to stable states.

In Figure 3-27, the initial value of pressure difference is close to 100 Pa, which is the same as the average value in the previous case. It is reasonable since the

damping items as well as the resistance loss are neglected; in addition, the simulations are all performed without fire. Therefore, even with different initial values of pressure difference, their ultimate values should remain the same.

It is noticed that the ultimate value of temperature in Figure 3-28 is close to the ambient temperature. It first increases because the pressure inside of the system fluctuates. It finally returns to the initial value (the temperature in the admission duct) after the pressure curve becomes stable.

3.4 Conclusion

The plots of different regimes all result in a stable state ultimately though with various inputs. In section 3.1, the system remains stable with different input environmental parameters. Next, in section 3.2, it is more reasonable to use the model with extinction compared to the one without extinction (especially when it belongs to under-ventilated regime). Thus, the model with flame extinction is preferred for further tests. In addition, it is noticed that the stable state maintains even with reversal flow phenomena during the ignition period. Moreover, in section 3.3, the oscillations in the preliminary model appear as expected, after applying Helmholtz oscillation theory. Furthermore, all the simulated results go well with the hand-calculated values; therefore, the preliminary model is quantitatively correct.

4 Validation tests (with prescribed fuel mass loss rate)

This chapter is to test and validate the simulation model. The prescribed mass loss rates are applied to the model, and then the numerical plots are compared with the experimental ones to test the model.

4.1 Validations by using prescribed fuel mass loss rate

This section is to validate the model by using the mass loss rate data measured by PRISME and then compare the values of other output variables with the corresponding experimental data.

4.1.1 Model Validation 1 (prescribed fuel mass loss rate, PRISME Source D1)

The experiment source named PRISME Source D1 is used in this case, combining with the model with no extinction. To note, the model with no extinction is only used here temporarily for a preliminary validation test study; the more reasonable model with extinction will be discussed and used in the following cases.

The initial conditions for the input parameters are listed here:

$r_{\text{adm}} = 7981.888\ (\text{m}^{-4}),\ r_{\text{ext}} = 12174.14\ (\text{m}^{-4})$
$P_0 = 101325\ (\text{Pa}),\ P(t_0) = P_0 + 50.0156(\text{Pa})$
$P_{\text{adm}}(t_0) = P_0 + 187.734\ (\text{Pa}),\ P_{\text{ext}}(t_0) = P_0 - 370.104\ (\text{Pa})$
$T(t_0) = 305.07\ (\text{K}),\ T_w(t_0) = 293\ (\text{K}),\ T_{\text{adm}} = 293\ (\text{K})$
$Y(t_0) = 23\%,\ Y_f(t_0) = 0\%$
$\Delta H_{\text{f}} = 44.56\ (\text{MJ/kg}),\ h = 15\ (\text{W} \cdot \text{m}^{-2} \cdot \text{K}^{-1})$
$\dot{m}_{\text{f}} = \dot{m}_{\text{f,exp}}$
$rs = 3.52,\ \gamma = 1.4$
$L = 10\ (\text{m}),\ S = 0.18\ (\text{m}^2),\ V = 120\ (\text{m}^3)$
$\dot{m}_{\text{adm}} = \dot{m}_{\text{ext}} = 0.1821\ (\text{kg/s})$

where $\dot{m}_{adm}$ and $\dot{m}_{ext}$ are obtained at steady state without fire.

To note, the initial values of pressure, temperature, etc. here are first processed by a no fire model. Therefore, they may change if the initial system is not stable. So are the situations in the following cases.

The output plots are listed as below:

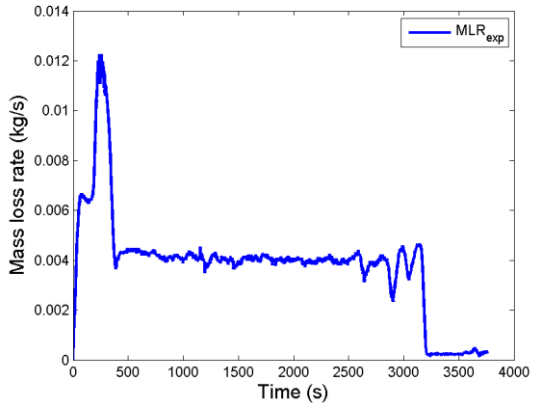

Figure 4-1 Time variation of mass loss rate, a validation test by using a prescribed mass loss rate (PRISME Source D1)

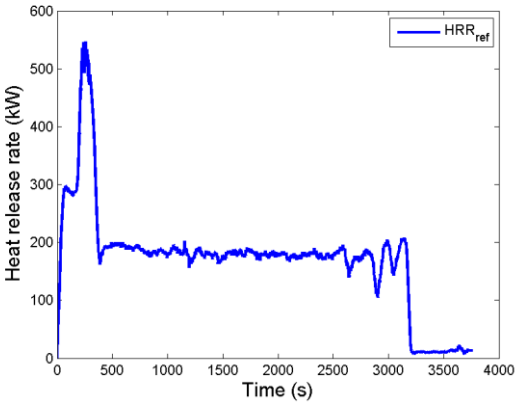

Figure 4-2 Time variation of heat release, a validation test by using a prescribed mass loss rate (PRISME Source D1)

In this case, the raw experimental data is disposed since the measurements were started before the initial experiment. The time range is set to be 3750 seconds long.

Figure 4-4 is the plot of input mass loss rate; Figure 4-5 is the plot of output heat release time, which has a similar tendency as Figure 4-4.

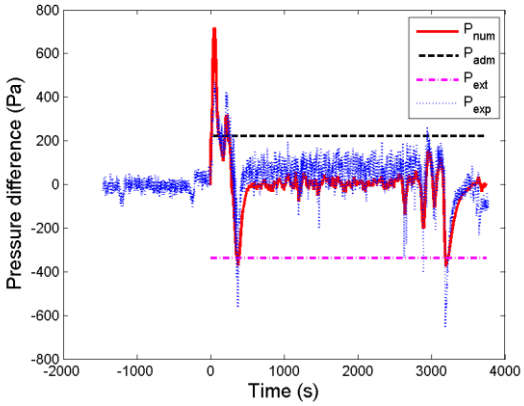

Figure 4-3 Time variation of pressure difference, a validation test by using a prescribed mass loss rate (PRISME Source D1)

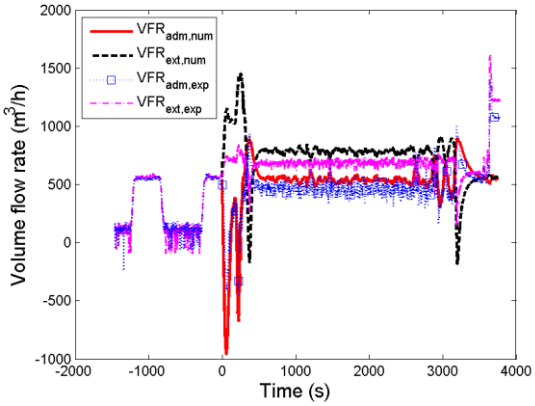

Figure 4-4 Time variation of volume flow rate, a validation test by using a prescribed mass loss rate (PRISME Source D1)

In these two plots, the numerical curves overall go well with the experimental ones. Their tendencies go well with each other; however, there are still some differences in the areas with severe fluctuation.

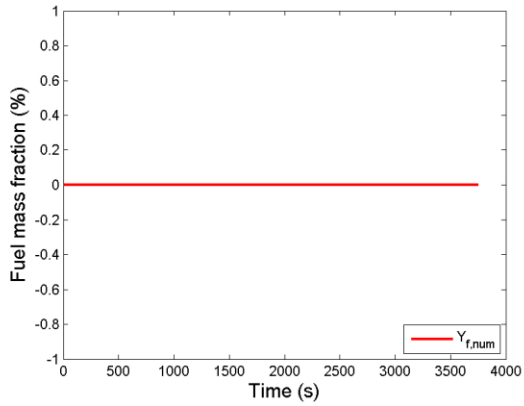

Figure 4-5 Time variation of fuel mass fraction, a validation test by using a prescribed mass loss rate (PRISME Source D1)

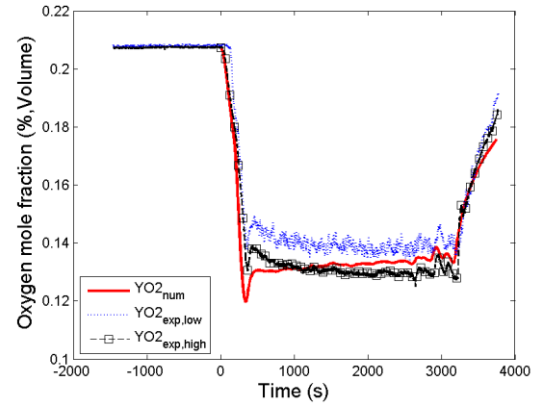

Figure 4-6 Time variation of oxygen mole fraction, a validation test by using a prescribed mass loss rate (PRISME Source D1)

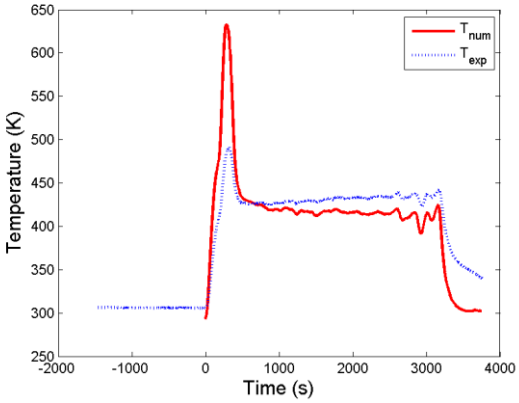

Figure 4-7 Time variation of temperature, a validation test by using a prescribed mass loss rate (PRISME Source D1)

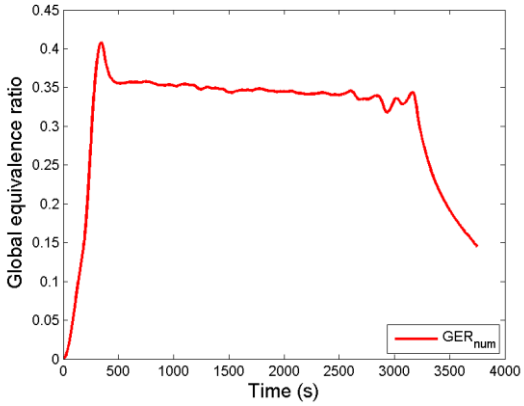

Figure 4-8 Time variation of global equivalence ratio, a validation test by using a prescribed mass loss rate (PRISME Source D1)

This case is an over-ventilation regime according to Figure 4-5 and Figure 4-8, because the fuel is all exhausted and value of global equivalence ratio is always less than 1. To plot Figure 4-6, the numerical oxygen mass fraction is changed into oxygen volume fraction in order for direct comparison with the experimental plot. In Figure 4-7, the average value of various groups of experimental data detected in different positions is calculated to plot the experimental curve.

4.1.2 Model Validation 2 (prescribed fuel mass loss rate, PRISME VSP S3)

The experiment source named PRISME VSP S3 is used here combined with the model, plus the designed critical value of oxygen mass fraction for flame extinction. The values of 0.10, 0.12 and 0.14 are chosen here.

The initial conditions for the input parameters are listed here:

$r_{\text{adm}} = 1976.787\ (\text{m}^{-4}),\ r_{\text{ext}} = 3396.091\ (\text{m}^{-4})$

$P_0 = 101325\ (\text{Pa}),\ P(t_0) = P_0 - 53.90(\text{Pa})$

$P_{\text{adm}}(t_0) = P_0 + 383.984\ (\text{Pa}),\ P_{\text{ext}}(t_0) = P_0 - 693.352\ (\text{Pa})$

$T(t_0) = 301.25\ (\text{K}),\ T_w(t_0) = 293\ (\text{K}),\ T_{\text{adm}} = 293\ (\text{K})$

$Y(t_0) = 23\%,\ Y_f(t_0) = 0\%$

$\Delta H_{\text{f}} = 44.56\ (\text{MJ/kg}),\ h = 15\ (\text{W}\cdot\text{m}^{-2}\cdot\text{K}^{-1})$

$\dot{m}_{\text{f}} = \dot{m}_{\text{f,exp}}$

$rs = 3.52,\ \gamma = 1.4$

$L = 10\ (\text{m}),\ S = 0.18\ (\text{m}^2),\ V = 120\ (\text{m}^3)$

$\dot{m}_{\text{adm}}(t_0) = \dot{m}_{\text{ext}}(t_0) = 0.4898\ (\text{kg/s})$

where $\dot{m}_{\text{adm}}$ and $\dot{m}_{\text{ext}}$ are obtained at steady state without fire.

The output plots are listed as below:

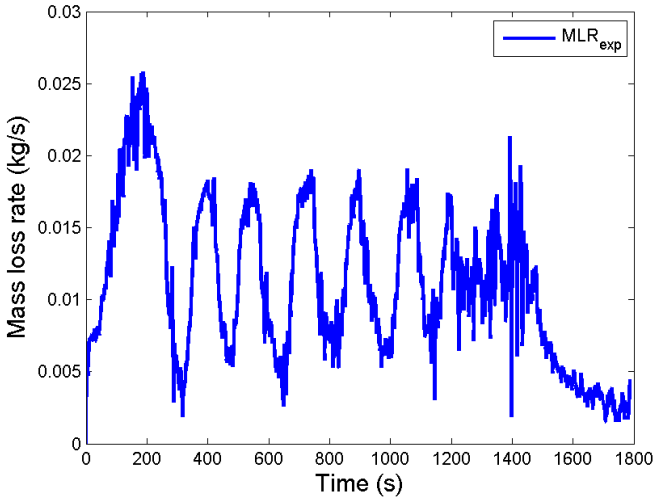

Figure 4-9 Time variation of fuel mass loss rate, a validation test by using a prescribed mass loss rate (PRISME VSP S3)

In this section, six cases with various values of *FEF* are implemented. However, their plots of fuel mass loss rate are the same, since they are all input instead of being calculated

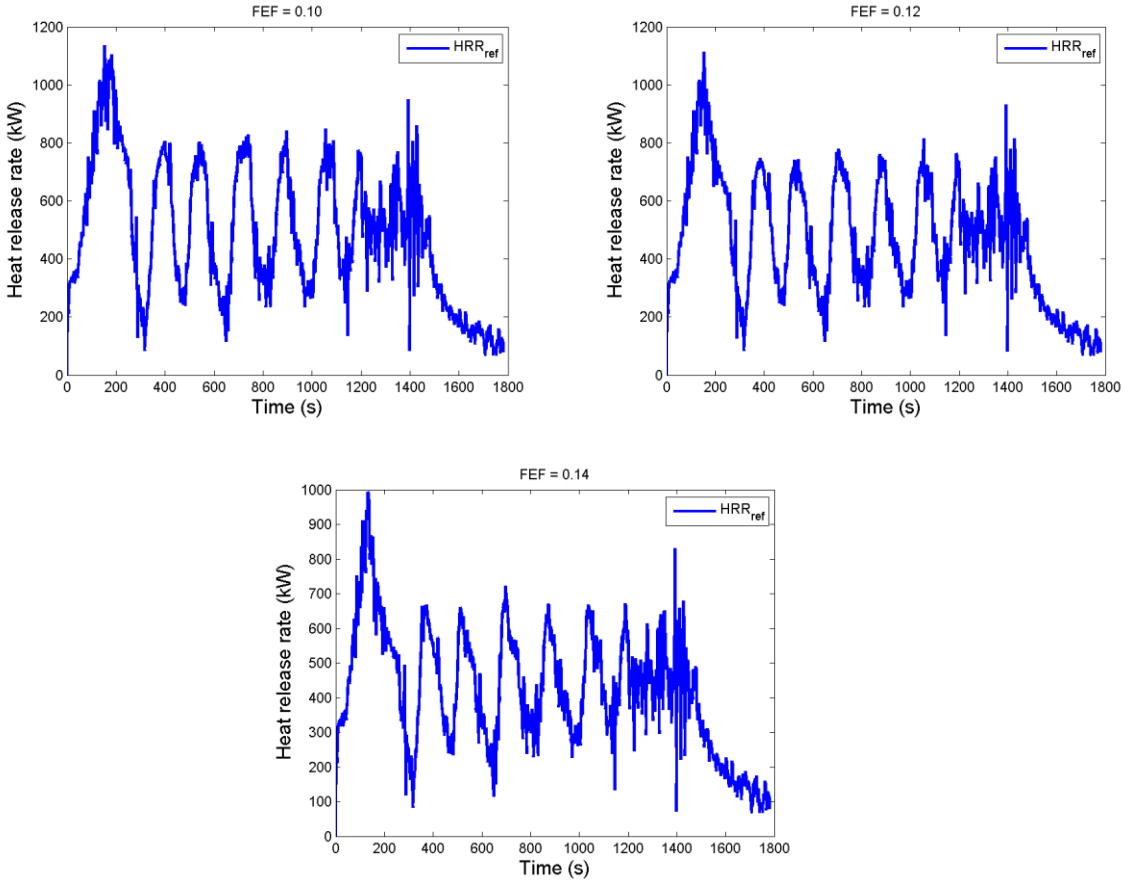

Figure 4-10 Time variation of heat release rate with various FEF s, a validation test by using a prescribed mass loss rate (PRISME VSP S3)

The corresponding values in different curves become smaller as the FEF increases. This is reasonable because the flame will extinct earlier with a higher value of FEF , therefore, it cannot release so much heat as expected. Both Figure 4-9 and Figure 4-10 fluctuate until the end of the combustion.

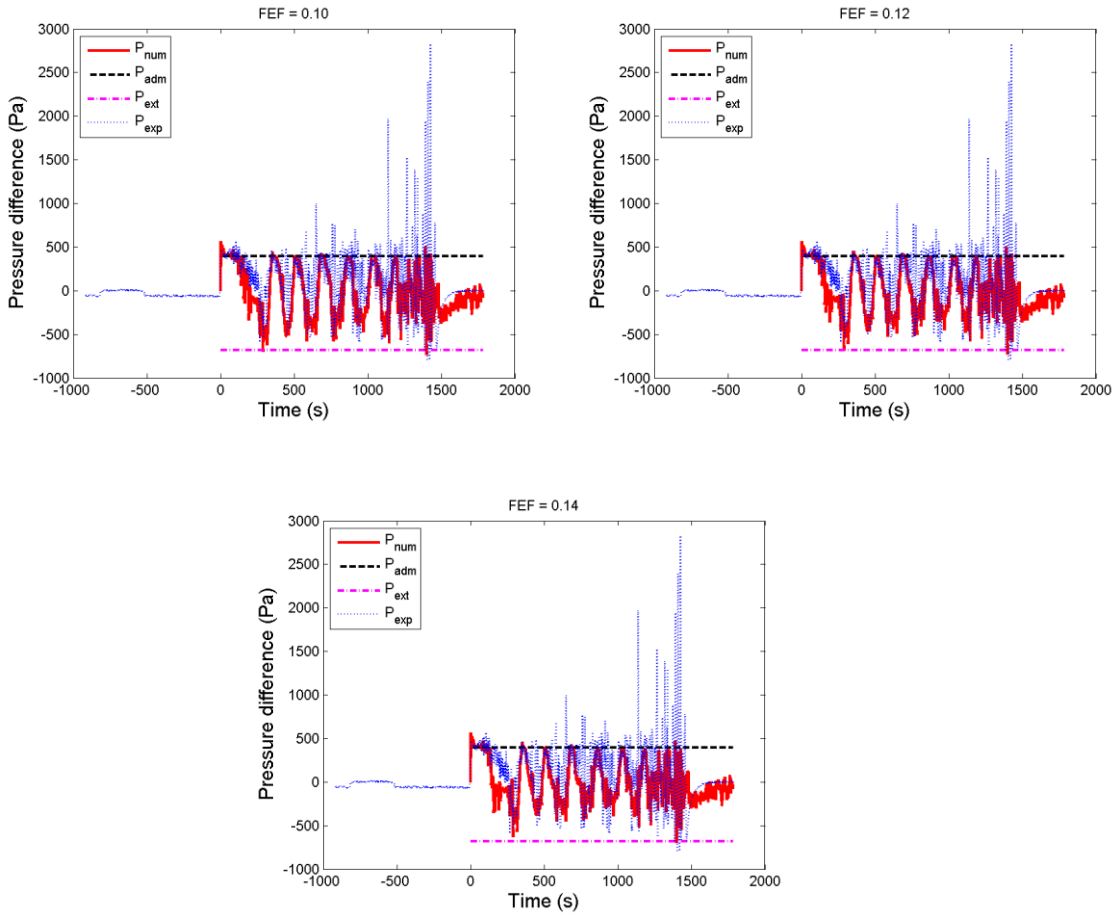

Figure 4-11 Time variation of pressure difference with various FEF s, a validation test by using a prescribed mass loss rate (PRISME VSP S3)

When $FEF = 0.12$, the numerical curve fits the experimental one best, especially by comparing with the curve plotted by suing $FEF = 0.14$ for the starting part, and with the curve plotted by using $FEF = 0.10$ for the middle part.

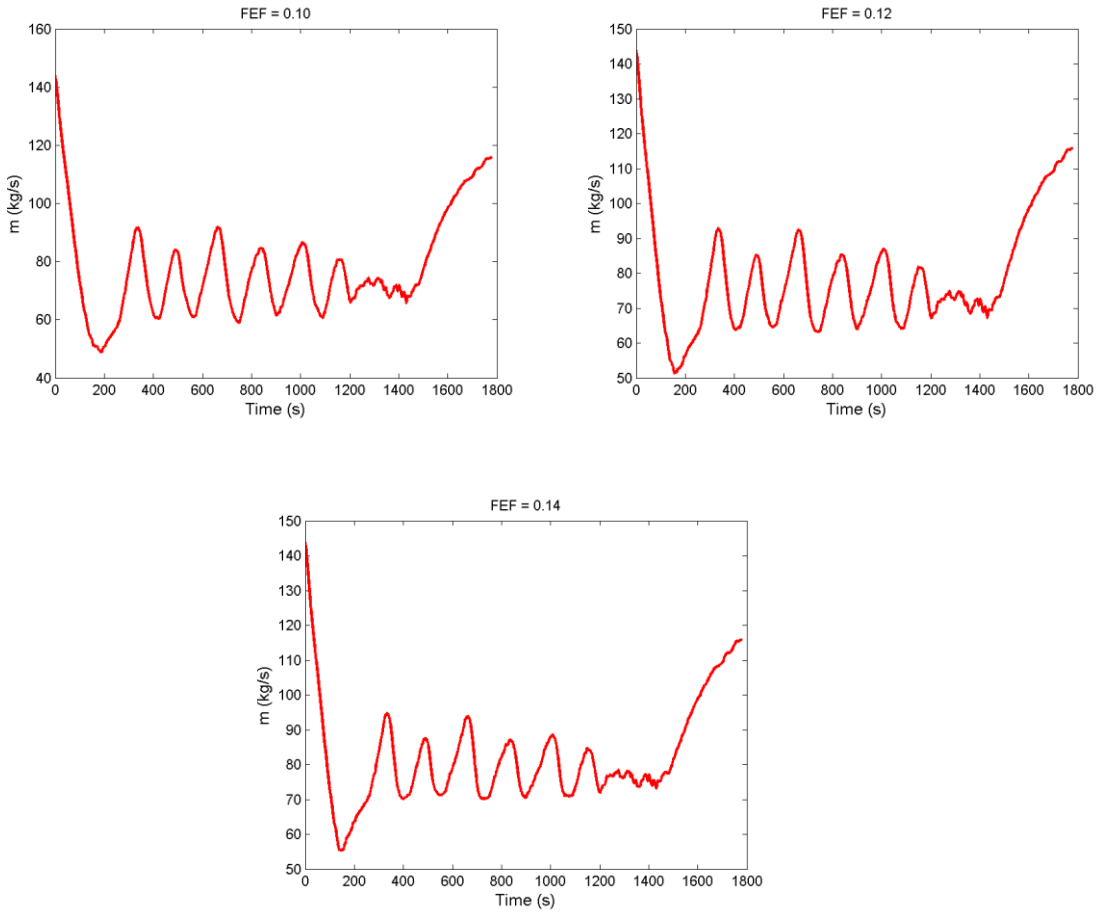

Figure 4-12 Time variation of total mass difference with various FEF s, a validation test by using a prescribed mass loss rate (PRISME VSP S3)

The average value of total mass variation gets larger by implementing the extinction situation; this is because less fuel is consumed as FEF increases. In the end, the plots keep increasing because both oxygen and fuel are no more consumed by the reaction.

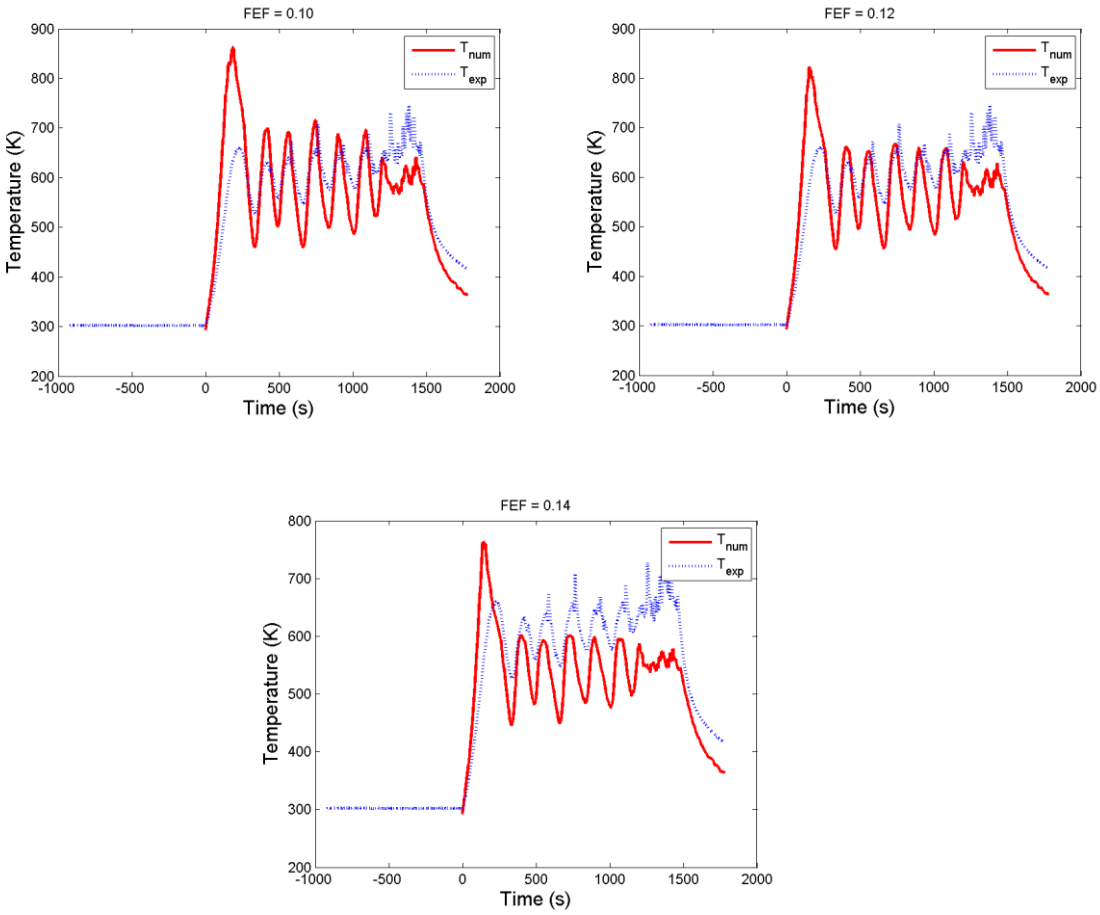

Figure 4-13 Time variation of temperature with various *FEF* s, a validation test by using a prescribed mass loss rate (PRISME VSP S3)

These plots are the variations of temperatures along with the time, and they show that 0.14 may not be a good choice for *FEF* , since the numerical curve in the last plot does not go well with the experimental one.

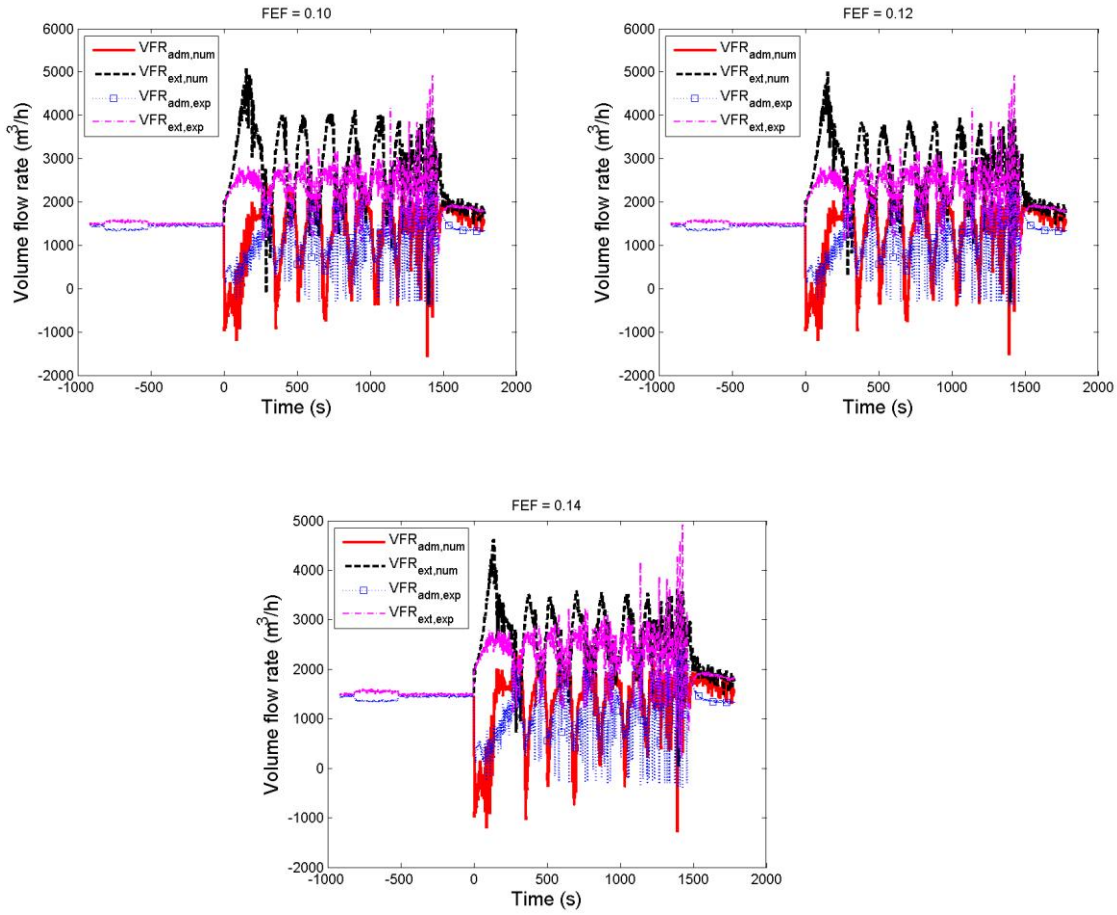

Figure 4-14 Time variation of volume flow rate with various FEF s, a validation test by using a prescribed mass loss rate (PRISME VSP S3)

The reverse flow appears since the initial pressure inside the compartment is higher. Meanwhile the flows have unstable oscillations due to the similar behavior of the prescribed mass flow rate. The directions of each inflow and outflow are different, however, they shares a similar time period.

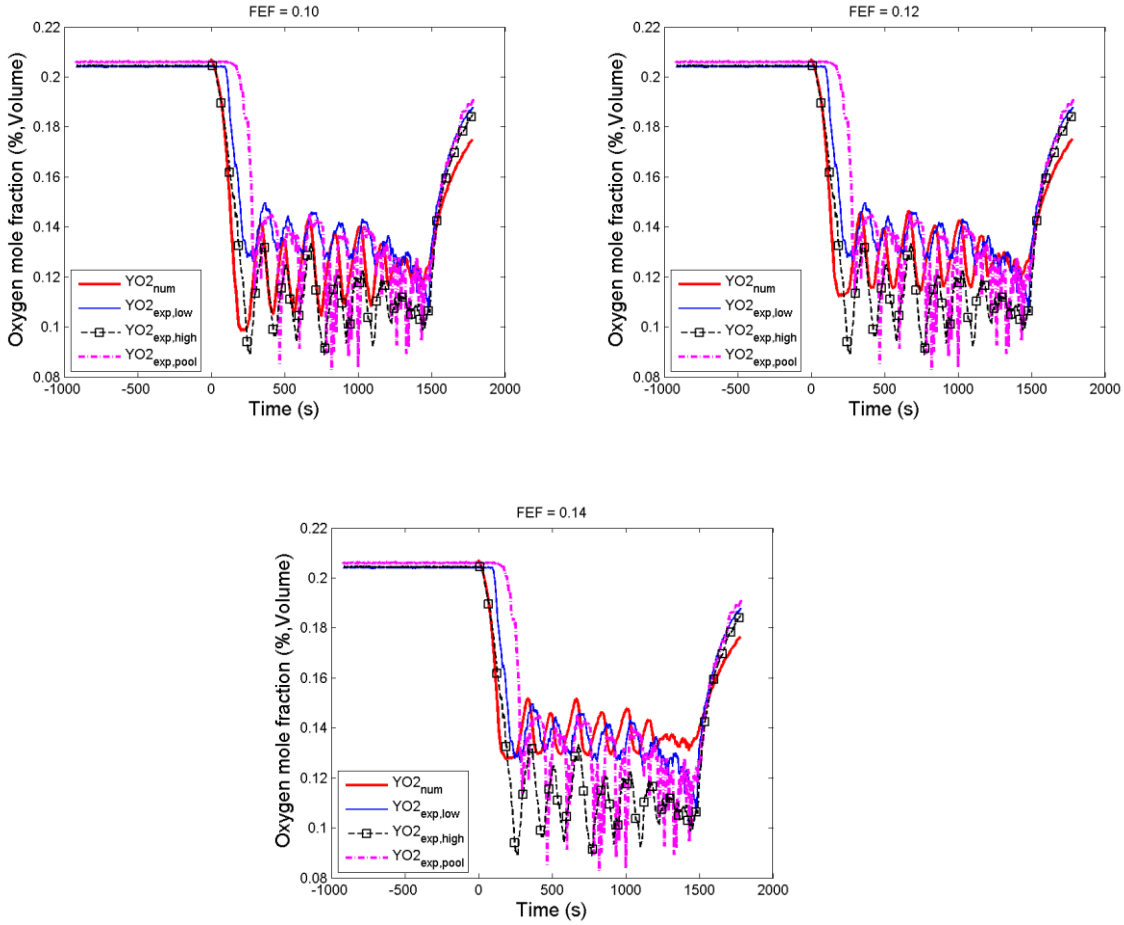

Figure 4-15 Time variation of oxygen mole fraction with various FEF s, a validation test by using a prescribed mass loss rate (PRISME VSP S3)

These curves first decrease because the oxygen is consumed to support the combustion; after that, they experience oscillations; in the end, they increase sharply because the combustion stops. The overall values in the numerical curve increase as FEF increases, because there is a higher critical value of oxygen mass fraction for flame extinction. Moreover, the periods of the oscillation here are close to those of the inflows and outflows in Figure 4-14.

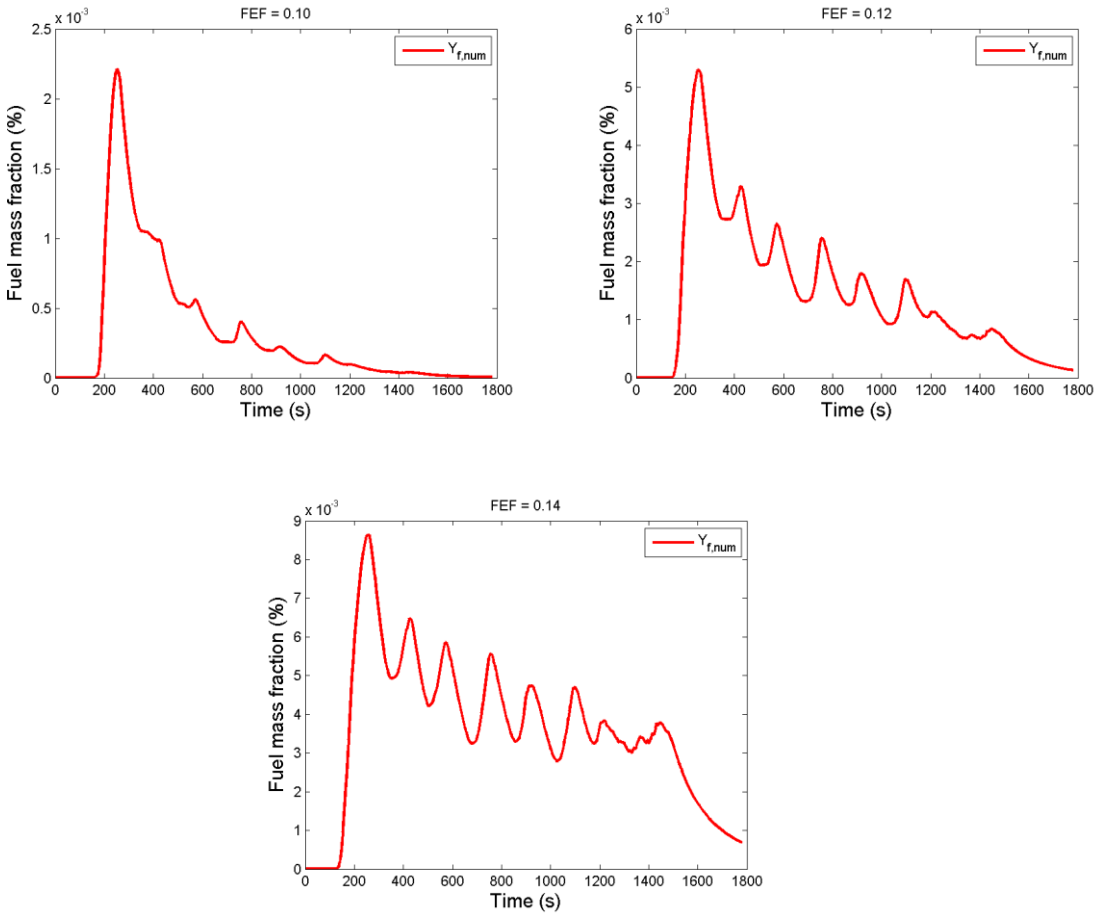

Figure 4-16 Time variation of fuel mass fraction with various FEF s, a validation test by using a prescribed mass loss rate (PRISME VSP S3)

There is less fuel remaining since there is a continuous oxygen supply to consume. However, the fuel remains non-zero before the end, since a critical value of oxygen mass fraction with flame extinction is used and it prevents the fuel to be used up. Similarly, the average amount of fuel mass fraction becomes larger as FEF increases.

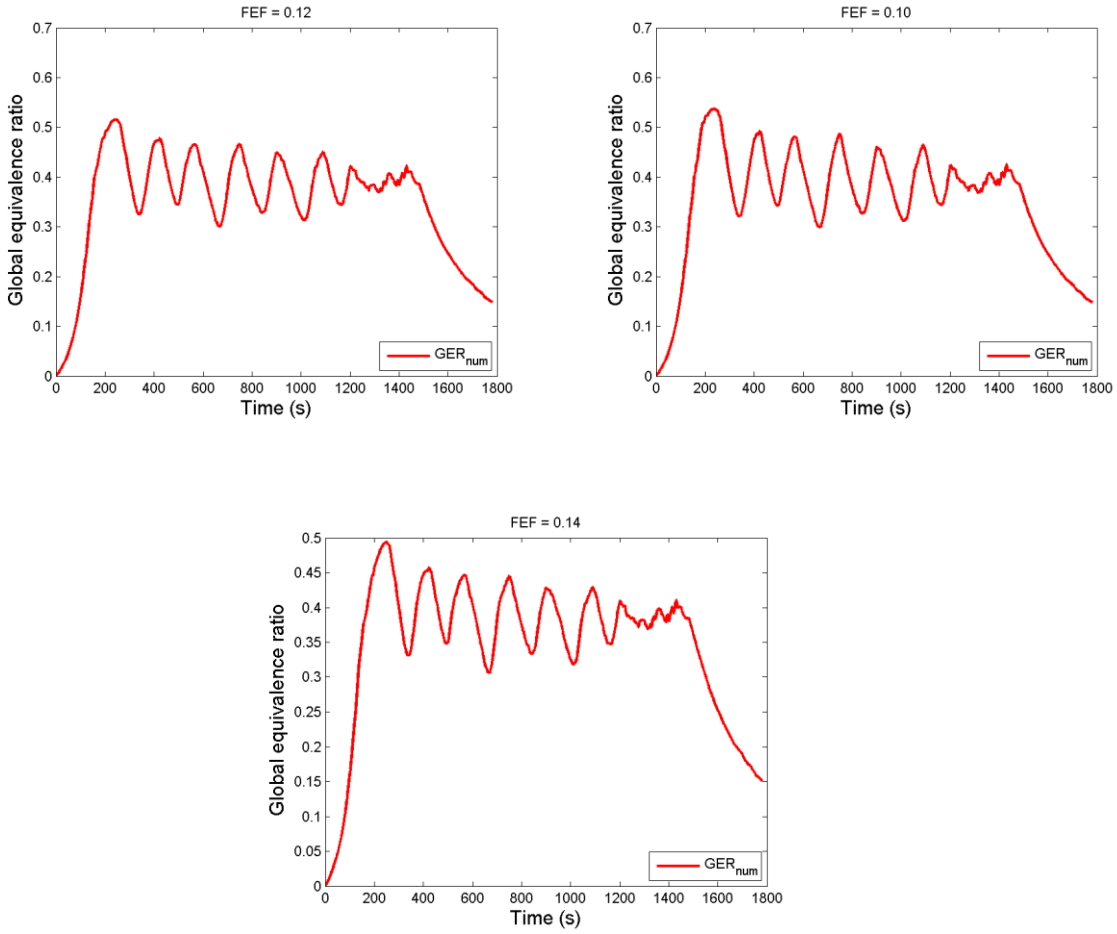

Figure 4-17 Time variation of equivalence ratio with various FEF s, a validation test by using a prescribed mass loss rate (PRISME VSP S3)

The value of equivalent ratio decreases as FEF increases. Despite the unstable behavior throughout the test, the value of the equivalence ratio is always less than 1, which shows the system is over-ventilated.

4.2 Conclusion

In this chapter, the simulation plots go well with the experimental ones. Moreover, 3 different values of FEF are tested for the critical oxygen fraction of the model with extinction. According to the observation on the numerical plots, $FEF = 0.12$ seems to match the experimental results best and hence is to be selected for the extinction model.

5 Validation tests (with simulated fuel mass loss rate)

To further study the unstable behavior, new mass loss rate inputs are created in this chapter, instead of using the prescribed ones from the experiments directly. Three parts are mainly involved in this chapter: the first section is to briefly introduce the new N-τ model, the second section is to verify the algorithm of the model by a simple test, and the third section is to couple oxygen fraction, temperature and admission mass flow rate with the mass loss rate and then to analyze the oscillations.

5.1 Brief introduction to the N-τ model

The study of unstable behavior in combustion has attracted people's attention in the past decades. Especially, the connection between the flame and the environment conditions was observed and studied. Therefore, a series of corresponding models which describe the unstable combustion phenomenon were proposed. One of the basic models suggests that the unsteady combustion system can be solved by coupling with the wave amplitudes of the insert environment parameters. Moreover, instead of solely depending on these amplitudes, it is sufficient to regard a constant time delay between fuel source injection and combustion due to perturbations, chemical effects and so on[24][25]. Therefore, take the coupling between oxygen mass fraction and mass loss rate as an example, a simple time lag model, which is named N-τ model, is considered as:

$$\dot{m}_{\mathrm{f}}(t) = \overline{\dot{m}_{\mathrm{f}}} + N\left(Y_{\mathrm{O}_2}\left(t-\tau\right) - \overline{Y_{\mathrm{O}_2}}\right) \tag{5.1}$$

where $\overline{\dot{m}_f} = 0.01$ kg/s is the mean value of fuel mass loss rate; $\overline{Y_{O_2}} = 0.15$ is the mean value of oxygen mass fraction; N is the amplification factor that controls the magnitude of changes in fuel mass loss rate due to changes in oxygen mass fraction; and τ is the time delay between perturbations in oxygen mass fraction and fuel mass loss rate.

5.2 Verification by a simple test

In this section, the application to a simple function is tested to verify the algorithm which describes the time lag.

The initial conditions for the input parameters are listed here:

$$t = [0:0.1:10]$$
$$y_0 = e^{(-t)} \times t \times (10 - t)$$
$$\tau = 1 \text{ (s)}$$

The output plot is shown as below:

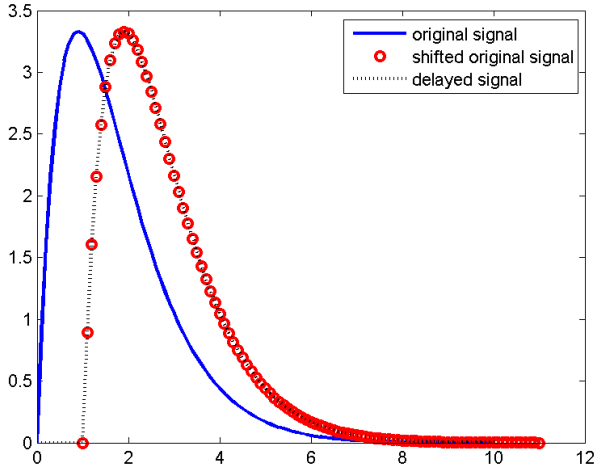

Figure 5-1 Time variation of time with a signal in different states, a simple verification test

Figure 5-1 consists of three curves, the first solid line represents the original signal; the second one plotted with circles shows the positions of the points (which constitutes the first curve) after being shifted along the x axis; the last dotted curve is directly plotted by the algorithm to be tested. It is reasonable to believe the algorithm is acceptable in the test, since the dotted curve plotted by the algorithm overlaps with the points which are directly shifted from the original plot.

5.3 Coupling oxygen fraction with mass loss rate

5.3.1 Model validation 3 (PRISME Source D1)

In this section, the N-τ method is applied into the coupling of oxygen mass fraction with mass loss rate. Experiment data from PRISME Source D1 package is used here.

The initial conditions for the input parameters are listed below:

$N = 0.4,\ \tau = 50$ s

$\overline{\mathrm{MLR}} = 0.004$ kg/s

$\overline{\mathrm{Y_{O_2}}} = 15\%$

$r_{\mathrm{adm}} = 7981.888\ (\mathrm{m}^{-4}),\ r_{\mathrm{ext}} = 12174.14\ (\mathrm{m}^{-4})$

$P_0 = 101325$ (Pa), $P(t_0) = P_0 + 50.0156$(Pa)

$P_{\mathrm{adm}}(t_0) = P_0 + 187.734$ (Pa), $P_{\mathrm{ext}}(t_0) = P_0 - 370.104$ (Pa)

$T(t_0) = 305.07$ (K), $T_w(t_0) = 293$ (K), T_{adm}=293 (K)

$Y(t_0) = 23\%,\ Y_f(t_0) = 0\%$

$\Delta H_{\mathrm{f}} = 44.56$ (MJ/kg), $h = 15\ (\mathrm{W \cdot m^{-2} \cdot K^{-1}})$

$\dot{m}_{\mathrm{f}} = \dot{m}_{\mathrm{f,exp}}$

$rs = 3.52,\ \gamma = 1.4$

$L = 10$ (m), $S = 0.18\ (\mathrm{m}^2)$, $V = 120\ (\mathrm{m}^3)$

$\dot{m}_{\mathrm{adm}} = \dot{m}_{\mathrm{ext}} = 0.1821$ (kg/s)

where the value of $\overline{\mathrm{MLR}}$ is the mean value of mass loss rate, and the value of $\overline{\mathrm{Y_{O_2}}}$ is the mean value of oxygen mass fraction (its corresponding oxygen mole fraction is slightly smaller, since the density of oxygen is larger than that of air). These two values mainly help to maintain the average values of the numerical mass loss rate and oxygen fraction in the reasonable ranges. They can be derived from the common sense combined with experimental plots, or from the numerical plots when $N = 0$ is set according to Equation 5.1.

Here are two plots for the mean values after setting $N = 0$:

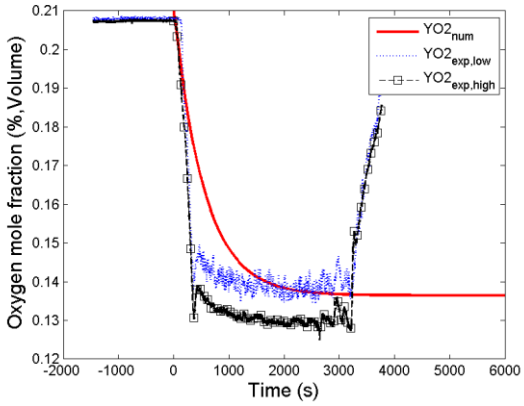

Figure 5-2 Time variation of oxygen mole fraction, a validation test of coupling oxygen faction with mass loss rate (PRISME Source D1, N=0)

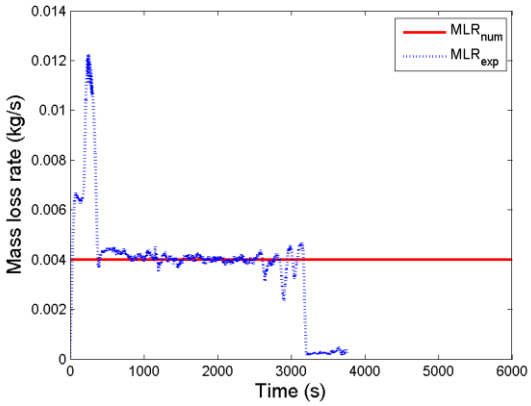

Figure 5-3 Time variation of mass loss rate a validation test of coupling oxygen faction with mass loss rate (PRISME Source D1, N=0)

It is obvious to see that the values of mass loss rate and oxygen mole fraction in the stable part of the experimental plots are close to those in $\overline{\mathrm{MLR}}$ and $\overline{\mathrm{Y_{O_2}}}$ separately. Therefore, the selected two values are acceptable.

The output plots for the case $N = 0.4$ are listed as below:

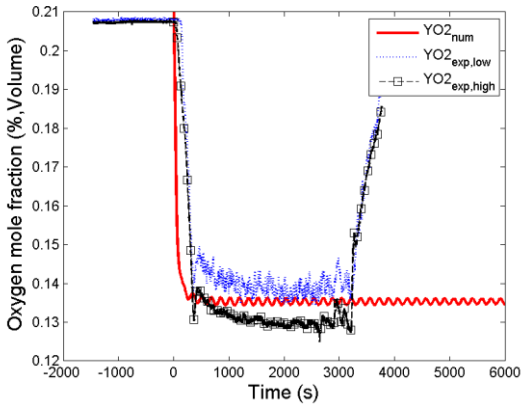

Figure 5-4 Time variation of oxygen mole fraction a validation test of coupling oxygen faction with mass loss rate (PRISME Source D1)

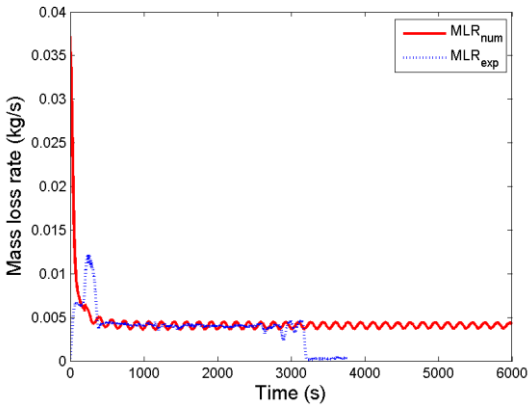

Figure 5-5 Time variation of mass loss rate, a validation test of coupling oxygen faction with mass loss rate (PRISME Source D1)

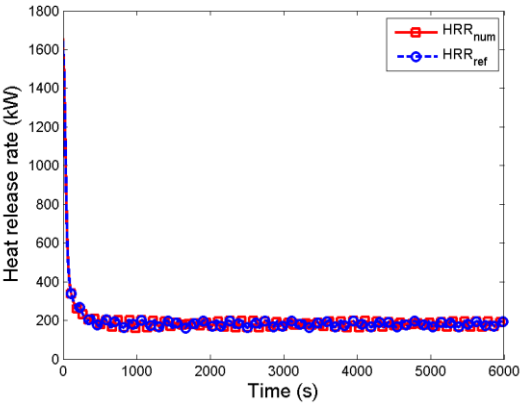

Figure 5-6 Time variation of heat release rate a validation test of coupling oxygen faction with mass loss rate (PRISME Source D1)

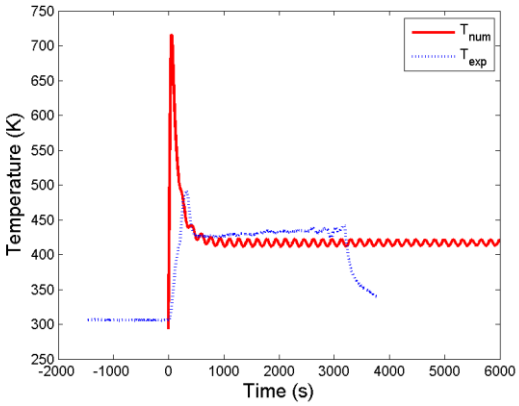

Figure 5-7 Time variation of temperature a validation test of coupling oxygen faction with mass loss rate (PRISME Source D1)

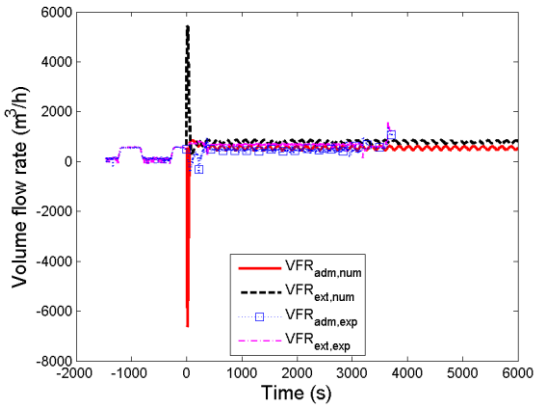

Figure 5-8 Time variation of volume flow fraction, a validation test of coupling oxygen faction with mass loss rate (PRISME Source D1)

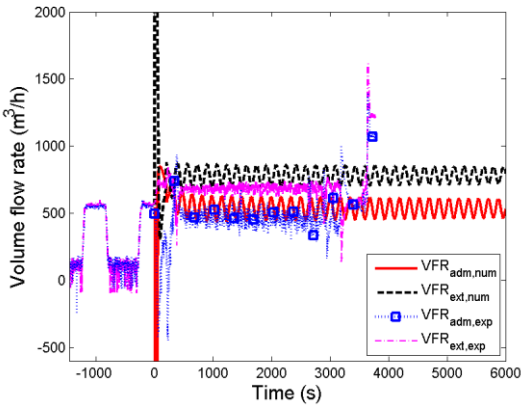

Figure 5-9 Time variation of volume flow fraction, a validation test of coupling oxygen faction with mass loss rate (PRISME Source D, zoomed in)

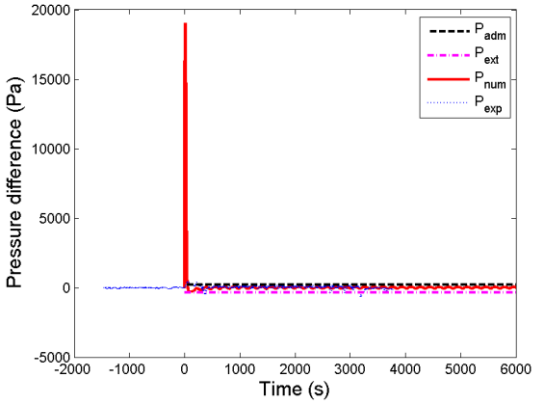

Figure 5-10 Time variation of pressure difference, a validation test of coupling oxygen faction with mass loss rate (PRISME Source D1)

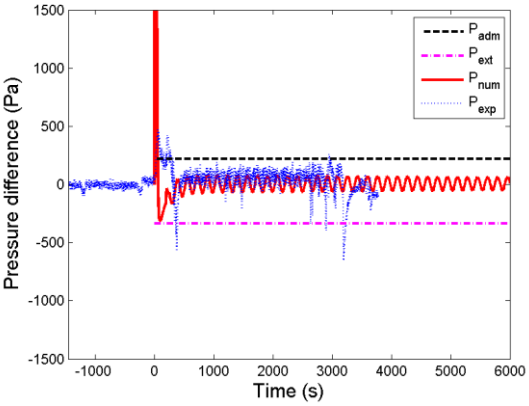

Figure 5-11 Time variation of pressure difference, a validation test of coupling oxygen faction with mass loss rate (PRISME Source D1, zoomed in)

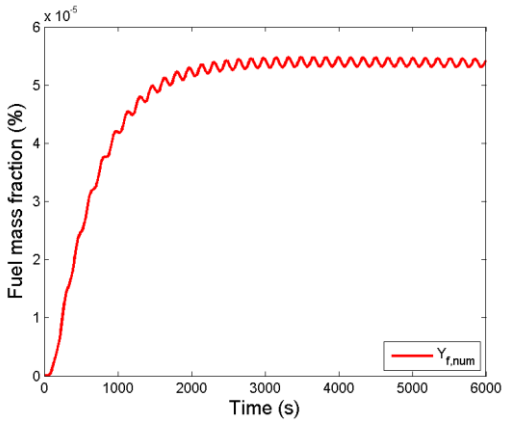

Figure 5-12 Time variation of mass fuel fraction, a validation test of coupling oxygen faction with mass loss rate (PRISME Source D1)

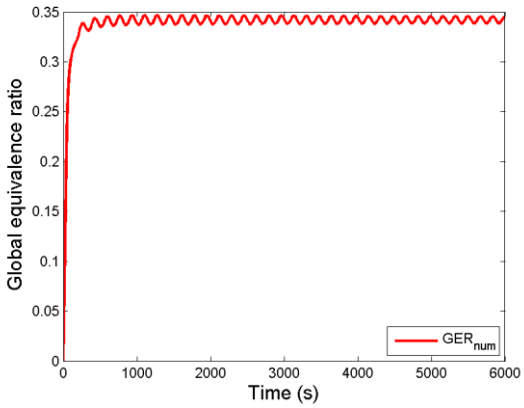

Figure 5-13 Time variation of global equivalence ratio, a validation test of coupling oxygen faction with mass loss rate (PRISME Source D1)

Figures 5-2 to 5-13 depict the change of the environment parameters along with the time. It is obvious that the PRISME Source D1 experiment shows a stable behavior; therefore the tiny fluctuations in the experimental plots are not easy to detect. Also, the average values for the rest parameters all match well with the corresponding experimental ones. However, obvious oscillations may be observed in the numerical plots by inputting specific values for N and τ (for example, this case). Therefore, a further oscillation study with more data collected from various cases is required for this coupling.

5.3.2 Model validation 4 (PRISME VSP S3)

In this section, the N-τ method is applied into the coupling of oxygen fraction with mass loss rate. Experiment data in PRISME VSP S3 package is used here.

The initial conditions for the input parameters are listed here:

$N = 0.4,\ \tau = 70$ s

$\overline{\text{MLR}} = 0.01$ kg/s

$\overline{\text{Y}_{\text{O}_2}} = 15\%$

$r_{\text{adm}} = 1976.787\ (\text{m}^{-4}),\ r_{\text{ext}} = 3396.091\ (\text{m}^{-4})$

$P_0 = 101325$ (Pa), $P(t_0) = P_0 - 53.90$(Pa)

$P_{\text{adm}}(t_0) = P_0 + 383.984$ (Pa), $P_{\text{ext}}(t_0) = P_0 - 693.352$ (Pa)

$\dot{m}_{\text{adm}}(t_0) = \dot{m}_{\text{ext}}(t_0) = 0.4898$ (kg/s)

$T(t_0) = 301.25$ (K), $T_w(t_0) = 293$ (K), T_{adm}=293 (K)

$Y(t_0) = 23\%,\ Y_f(t_0) = 0\%$

$\Delta H_{\text{f}} = 44.56$ (MJ/kg), $h = 15\ (\text{W}\cdot\text{m}^{-2}\cdot\text{K}^{-1})$

$\dot{m}_{\text{f}} = \dot{m}_{\text{f,exp}}$

$rs = 3.52,\ \gamma = 1.4$

$L = 10$ (m), $S = 0.18\ (\text{m}^2)$, $V = 120\ (\text{m}^3)$

where the values of $\overline{\text{MLR}}$ and $\overline{\text{Y}_{\text{O}_2}}$ can be observed from the numerical plots when setting $N = 0$ (as before):

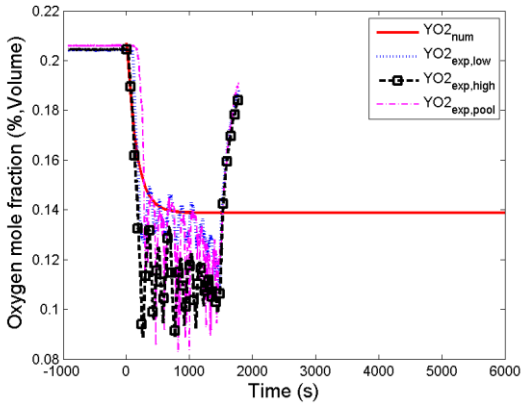

Figure 5-14 Time variation of oxygen mole fraction, a validation test of coupling oxygen faction with mass loss rate (PRISME VSP S3, N=0)

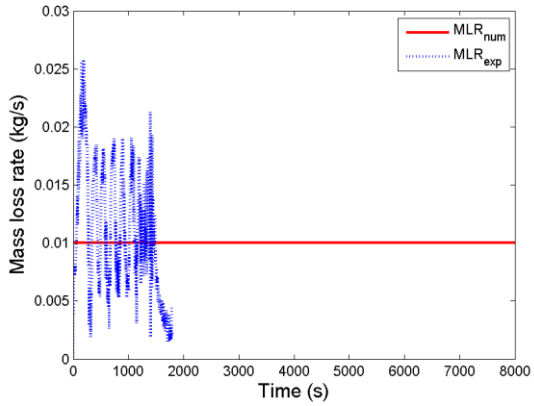

Figure 5-15 Time variation of mass loss rate, a validation test of coupling oxygen faction with mass loss rate (PRISME VSP S3, N=0)

It is obvious that the values of mass loss rate and oxygen mole fraction in the stable part of the experimental plots are close to those in $\overline{\text{MLR}}$ and $\overline{\text{Y}_{\text{O}_2}}$ separately. Therefore, the values here are acceptable.

The output plots for the case $N = 0.4$ are listed as below:

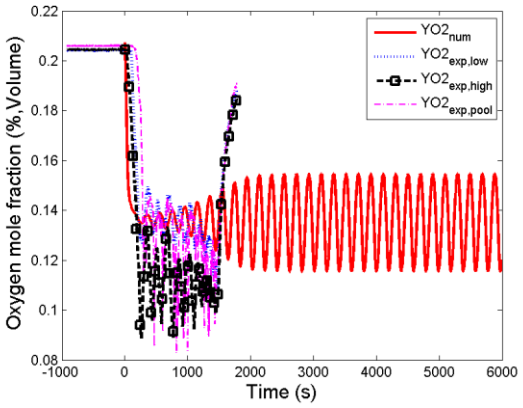

Figure 5-16 Time variation of oxygen mole fraction, a validation test of coupling oxygen faction with mass loss rate (PRISME VSP S3)

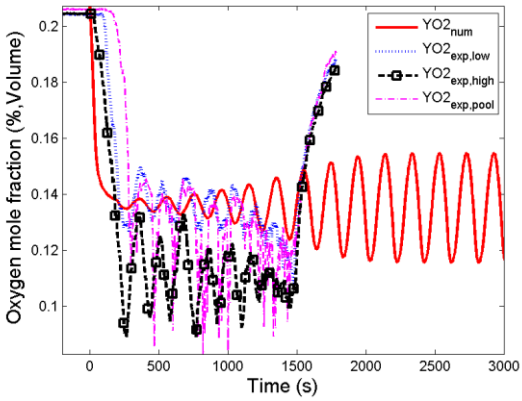

Figure 5-17 Time variation of oxygen mole fraction, a validation test of coupling oxygen faction with mass loss rate (PRISME VSP S3, zoomed in)

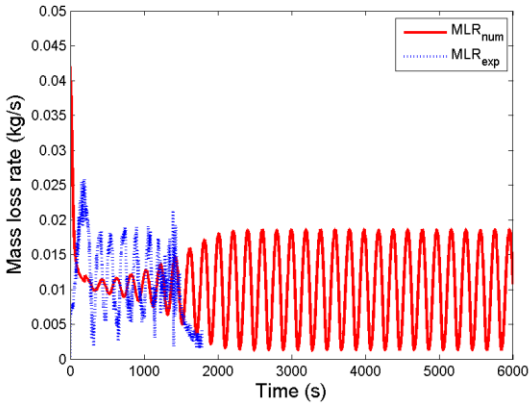

Figure 5-18 Time variation of mass loss rate, a validation test of coupling oxygen faction with mass loss rate (PRISME VSP S3)

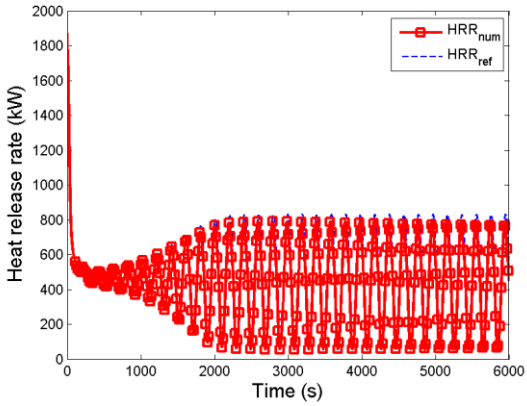

Figure 5-19 Time variation of heat release rate, a validation test of coupling oxygen faction with mass loss rate (PRISME VSP S3)

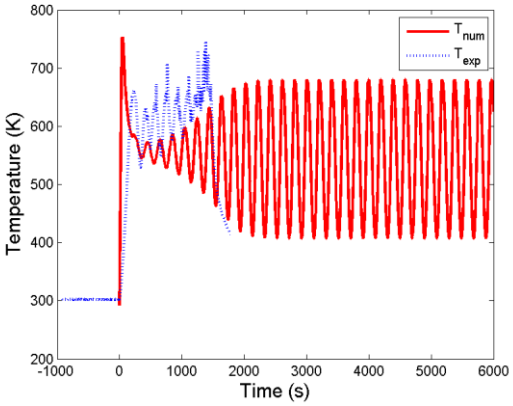

Figure 5-20 Time variation of temperature, a validation test of coupling oxygen faction with mass loss rate (PRISME VSP S3)

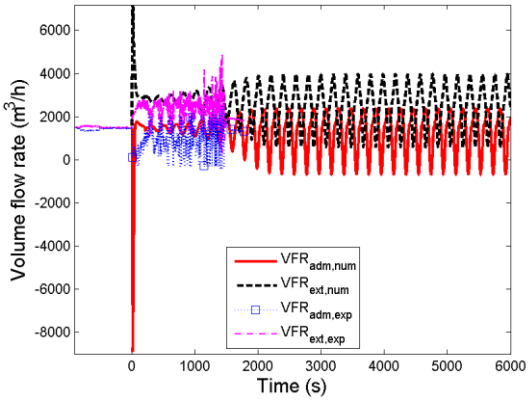

Figure 5-21 Time variation of volume flow rate, a validation test of coupling oxygen faction with mass loss rate (PRISME VSP S3)

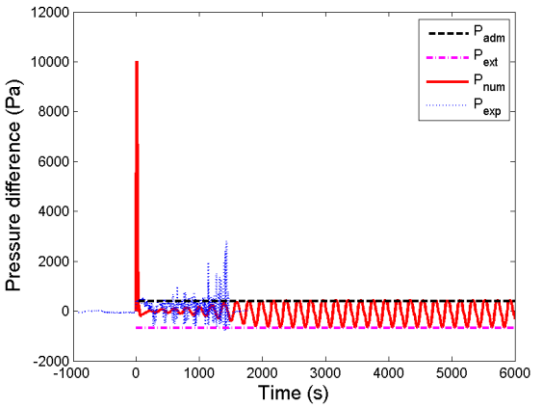

Figure 5-22 Time variation of pressure, a validation test of coupling oxygen faction with mass loss rate (PRISME VSP S3)

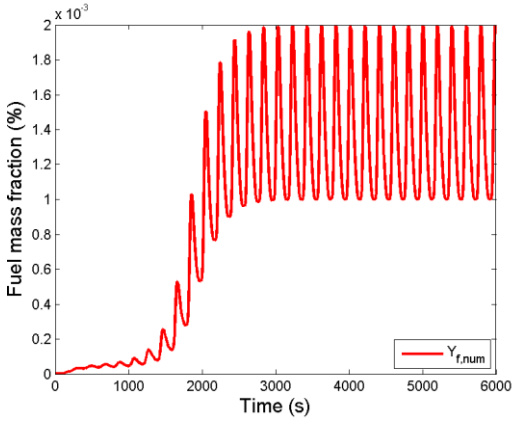

Figure 5-23 Time variation of fuel mass fraction, a validation test of coupling oxygen faction with mass loss rate (PRISME VSP S3)

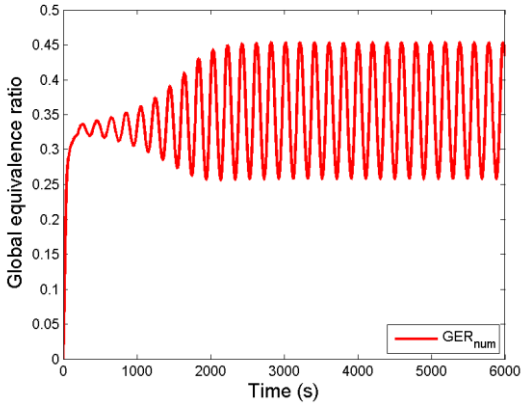

Figure 5-24 Time variation of global equivalence ratio, a validation test of coupling oxygen faction with mass loss rate (PRISME VSP S3)

Figure 5-16 and 5-17 depict the changes of oxygen mole (volume) fraction along with the time, which are essential during this coupling according to Equation (5.1). The amplitude of numerical curve (after 2000 s) is slightly larger than that of the experimental plot, however, their period matches well. To note, the middle part of the experimental plot is selected for the frequency and amplitude analysis, since it is stable there.

Mass loss rates in Figure 5-18 match well with each other. Heat release rates are compared in Figure 5-19, and two curves overall match well with each other; however, they do not exactly overlap with each other, since the extinction model is only applied to the one with the square symbols. Therefore, the extinction model impacts the simulation here.

The changes of pressure difference, volume flow rate and temperature are shown from Figures 5-20 to 5-22. Their periods match well, but the average value of the amplitude of the numerical curve is slightly larger compared to the experimental

ones. This is acceptable, since the differences are not that large, and we may modify the input values to decrease the amplitude.

Therefore, the model is overall acceptable; however, more values of N and τ should be tested for further oscillation analysis.

5.4 Coupling temperature with mass loss rate

According to the Section 5.3 above, it is more visualized to study the model by using PRISME VSP S3 package compared to PRISME Source D1 package, since the fluctuations shown by the experimental plots are tiny in the PRISME Source D1 scenario. Therefore, the data from PRISME VSP S3 package is preferred for the model validations first in the following couplings.

In this section, the N-τ method is applied into the coupling of oxygen fraction with temperature. Experimental data from PRISME VSP S3 package is used here.

$$\dot{m}_{\mathrm{f}}(t) = \overline{\dot{m}_{\mathrm{f}}} + N\left(T\left(t-\tau\right) - \overline{T}\right) \tag{5.2}$$

5.4.1 Model validation 5 (PRISME VSP S3)

Some initial conditions for the input parameters are listed here (others are the same as those used in Section 5.3.2:

$N = 0.00005,\ \tau = 300$ s
$\overline{\mathrm{MLR}} = 0.01$ kg/s
$\overline{\mathrm{T}} = 542$ K
$t\_\mathrm{switch} = 180$ s

where the values of $\overline{\mathrm{MLR}}$ and $\overline{\mathrm{Y_{O_2}}}$ can be observed from the numerical plots below when setting $N = 0$. $t_$switch is a compulsive time which control the starting time of

$N-\tau$ model's application. It is because the situation of this coupling is different from that of the previous coupling of oxygen mole fraction with mass loss rate. Take the experimental plots of time variation of temperature and oxygen mole fraction below as examples: In the starting time of the plot of temperature, the value keeps increasing, that is to say, it cannot reach its mean at the very beginning of the experiment. Therefore, it is necessary to set a time range - t_switch - to confirm the starting temperature (after N-τ model is applied) to be no less than $\overline{\mathrm{T}}$.

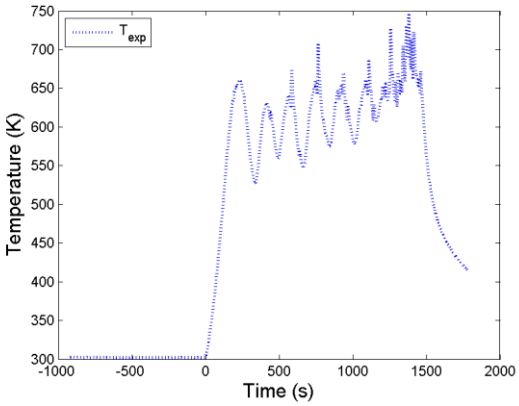

Figure 5-25 Time variation of temperature, (PRISME VSP S3)

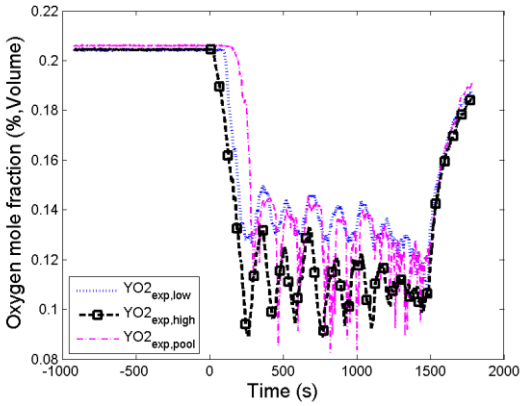

Figure 5-26 Time variation of oxygen mole fraction, (PRISME VSP S3)

Similarly, the values of $\overline{\mathrm{MLR}}$ and $\overline{\mathrm{Y_{O_2}}}$ can be observed from the numerical plots when setting $N=0$:

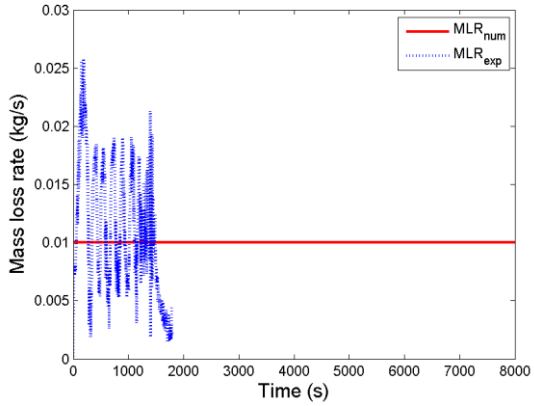

Figure 5-27 Time variation of mass loss rate, a validation test of coupling temperature with mass loss rate (PRISME VSP S3, N=0)

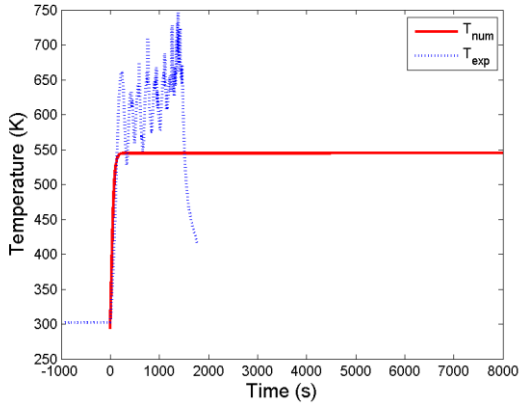

Figure 5-28 Time variation of temperature, a validation test of coupling temperature with mass loss rate (PRISME VSP S3, N=0)

The values of mass loss rate and temperature in the stable part of experimental plots are close to those in $\overline{\mathrm{MLR}}$ and $\overline{\mathrm{T}}$ separately. Therefore, the assumed input values are acceptable.

The output plots for the case when $N = 0.00005$ are listed as below:

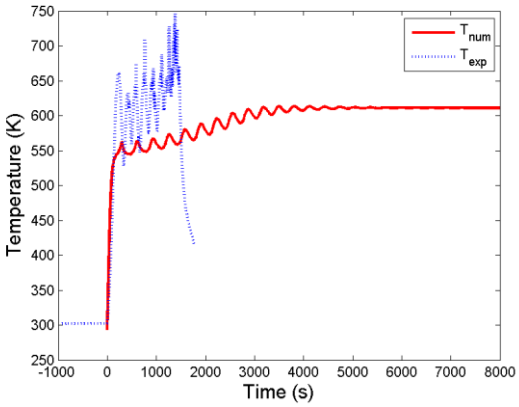

Figure 5-29 Time variation of temperature, a validation test of coupling temperature with mass loss rate (PRISME VSP S3, N=0.00005)

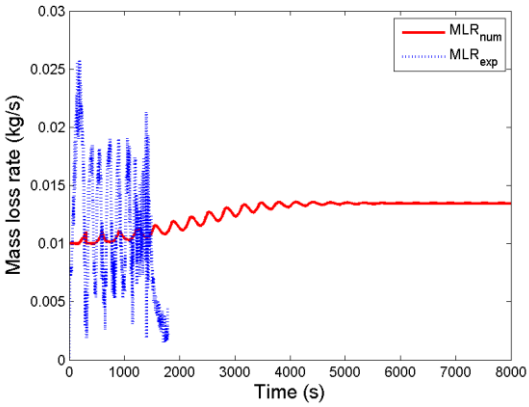

Figure 5-30 Time variation of mass loss rate, a validation test of coupling temperature with mass loss rate (PRISME VSP S3, N=0.00005)

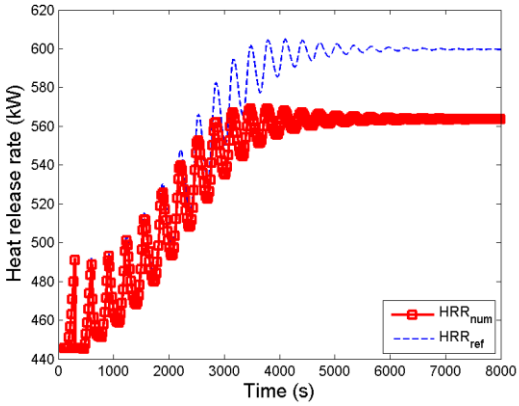

Figure 5-31 Time variation of heat release rate, a validation test of coupling temperature with mass loss rate (PRISME VSP S3, N=0.00005)

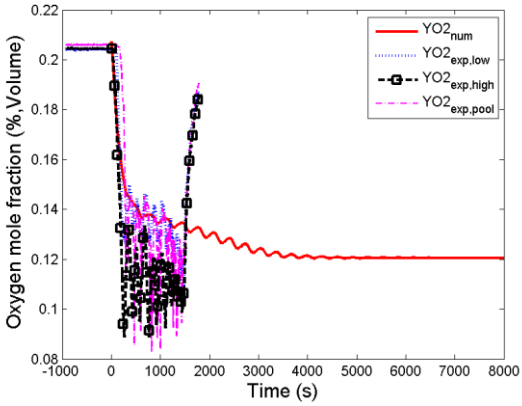

Figure 5-32 Time variation of oxygen mole fraction, a validation test of coupling temperature with mass loss rate (PRISME VSP S3, N=0.00005)

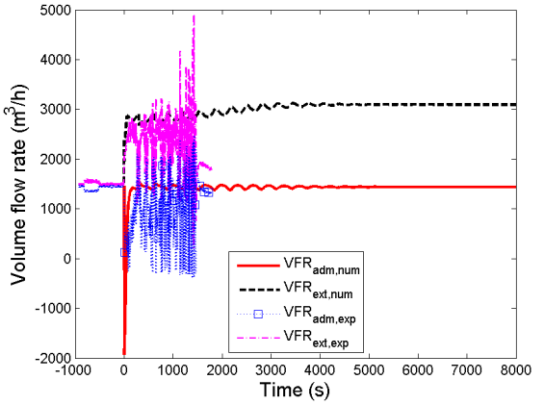

Figure 5-33 Time variation of volume flow rate, a validation test of coupling temperature with mass loss rate (PRISME VSP S3, N=0.00005)

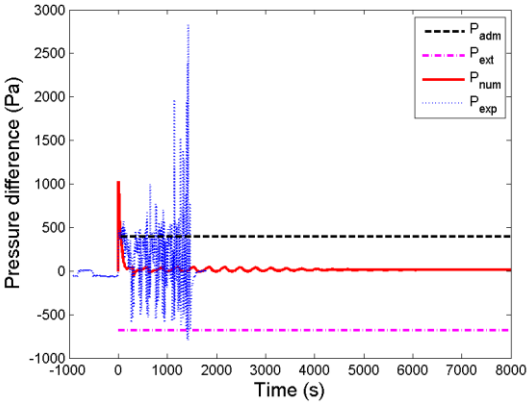

Figure 5-34 Time variation of pressure, a validation test of coupling temperature with mass loss rate (PRISME VSP S3, N=0.00005)

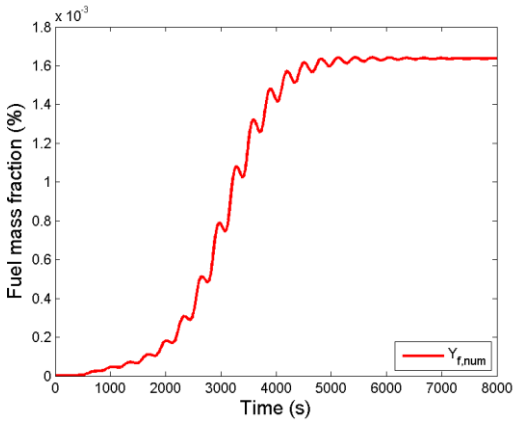

Figure 5-35 Time variation of fuel mass fraction, a validation test of coupling temperature with mass loss rate (PRISME VSP S3, N=0.00005)

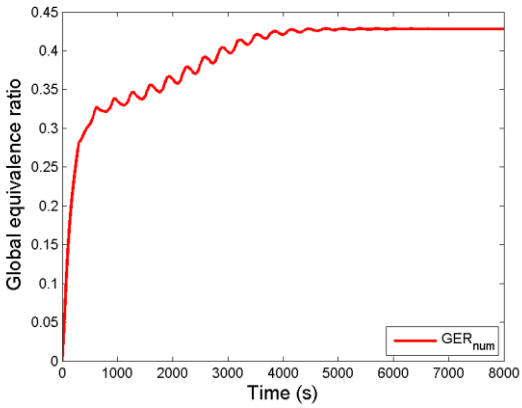

Figure 5-36 Time variation of global equivalence ratio, a validation test of coupling temperature with mass loss rate (PRISME VSP S3, N=0.00005)

This is a typical case of this coupling (where $\overline{\text{MLR}}$, $\overline{\text{T}}$ and t_switch are fixed). It is obvious to find that there is always decay for each oscillation, even though larger values of N and τ are tested. It is hard to analyze the oscillations here since there are no stable amplitudes or periods.

5.4.2 Model validation 6 (PRISME VSP S3)

The values of $\overline{\text{MLR}}$, $\overline{\text{T}}$ and t_switch are changed in this section. The initial conditions for the input parameters are listed here (others are the same as what appear in Section 5.3.2):

$N = 0.002,\ \tau = 100$ s
$\overline{\text{MLR}} = 0.013$ kg/s
$\overline{\text{T}} = 542$ K
$t\_\text{switch} = 180$ s

First check the values of $\overline{\text{MLR}}$, $\overline{\text{T}}$ and t_switch as before by setting $N = 0$:

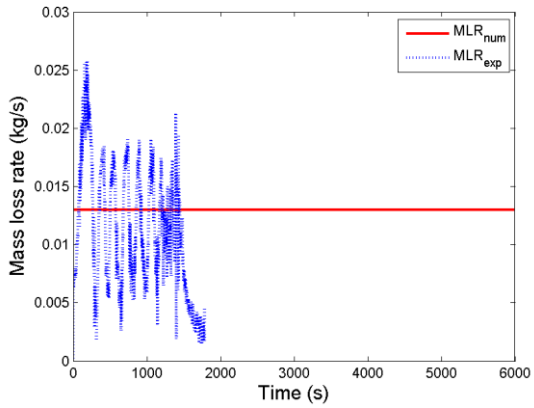

Figure 5-37 Time variation of mass loss rate, a validation test of coupling temperature with mass loss rate (PRISME VSP S3, N = 0)

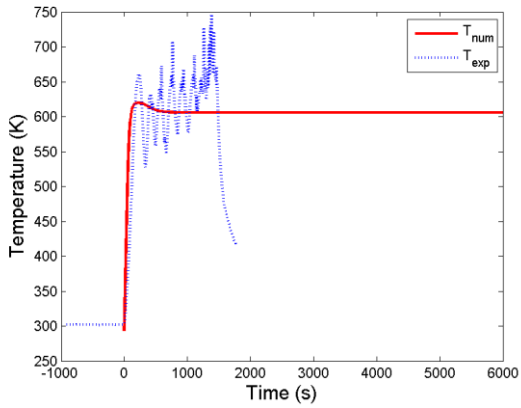

Figure 5-38 Time variation of temperature, a validation test of coupling temperature with mass loss rate (PRISME VSP S3, N = 0)

These two plots shows the initial inputs above are acceptable.

The output plots for the case $N = 0.002$ are listed as below:

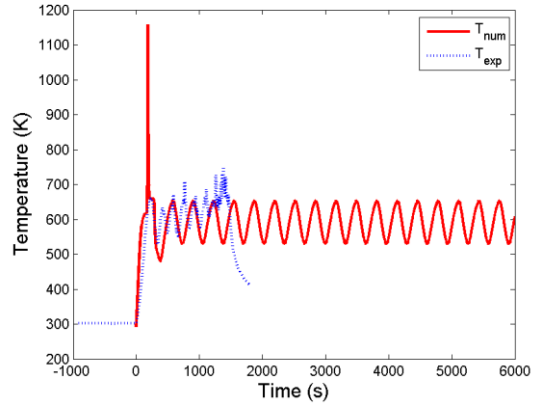

Figure 5-39 Time variation of temperature, a validation test of coupling temperature with mass loss rate (PRISME VSP S3, N=0.002)

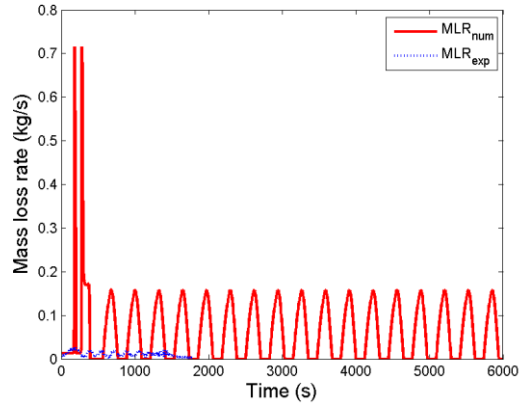

Figure 5-40 Time variation of mass loss rate, a validation test of coupling temperature with mass loss rate (PRISME VSP S3, N=0.002)

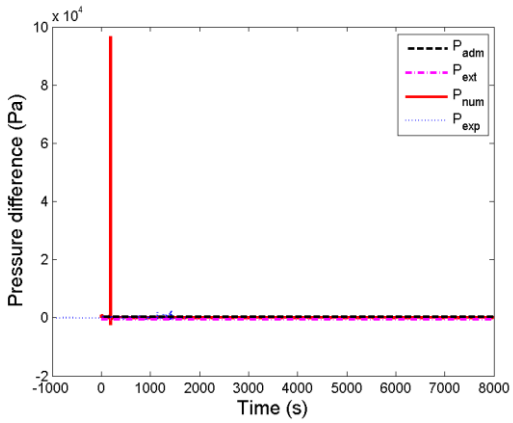

Figure 5-41 Time variation of heat release rate, a validation test of coupling temperature with mass loss rate (PRISME VSP S3, N=0.002)

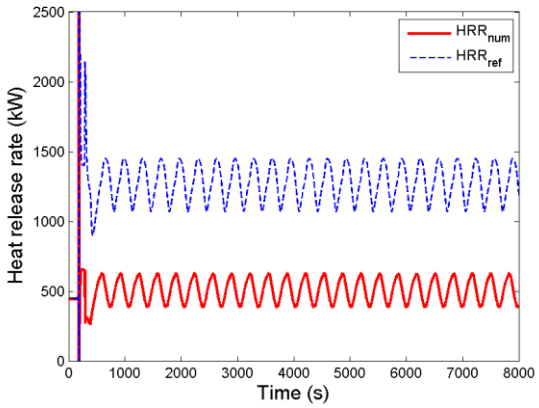

Figure 5-43 Time variation of heat release rate, a validation test of coupling temperature with mass loss rate (PRISME VSP S3, N=0.002, zoomed in)

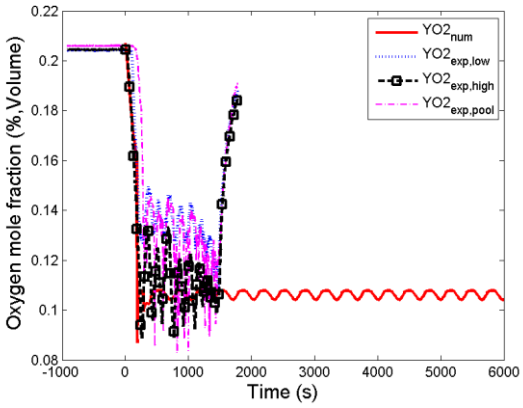

Figure 5-42 Time variation of oxygen mole fraction, a validation test of coupling temperature with mass loss rate (PRISME VSP S3, N=0.002)

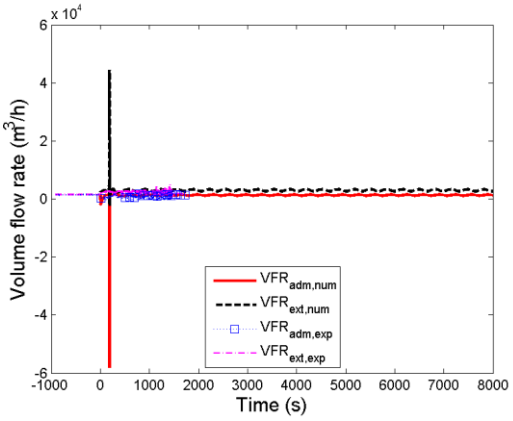

Figure 5-44 Time variation of volume flow rate, a validation test of coupling temperature with mass loss rate (PRISME VSP S3, N=0.002)

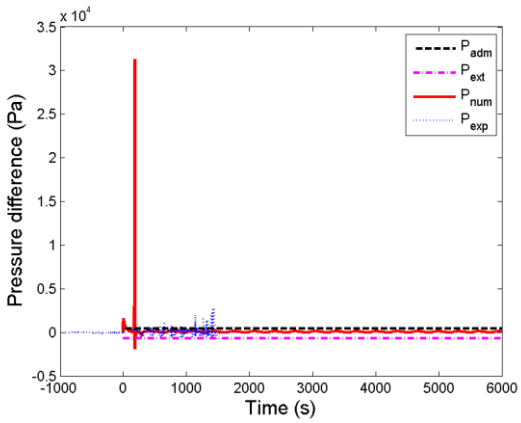

Figure 5-45 Time variation of pressure, a validation test of coupling temperature with mass loss rate (PRISME VSP S3, N=0.002)

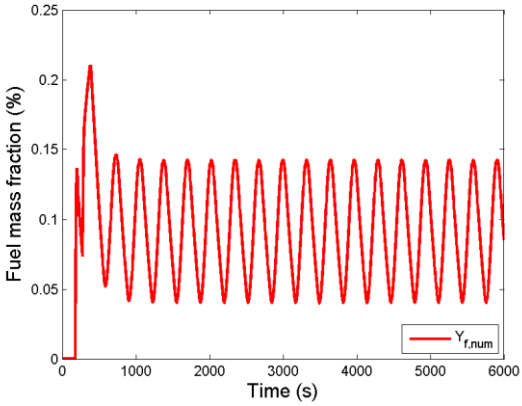

Figure 5-46 Time variation of fuel mass fraction, a validation test of coupling temperature with mass loss rate (PRISME VSP S3, N=0.002)

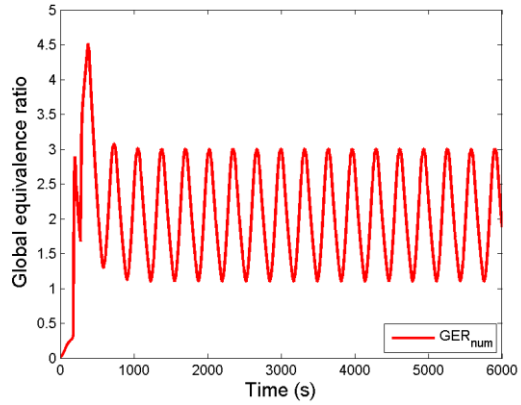

Figure 5-47 Time variation of global equivalence ratio, a validation test of coupling temperature with mass loss rate (PRISME VSP S3, N=0.002)

There are stable oscillations (without tendencies of decay) in this case; however, except the plot of temperature, the amplitudes of the numerical curves are obviously not in accordance with the experimental ones. Moreover, the average value of the global equivalence ratio is much higher than expected. Therefore, the codes for this coupling need to be modified before further oscillation study.

5.5 *Coupling mass flow rate (admission flow) with mass loss rate*

In this section, the N-τ method is applied into the coupling of admission flow rate with mass loss rate. Experimental data from PRISME VSP S3 package is used here.

$$\dot{m}_{\mathrm{f}}(t) = \overline{\dot{m}_{\mathrm{f}}} + N\left(\dot{m}_{\mathrm{adm}}(t-\tau) - \overline{\dot{m}_{\mathrm{adm}}}\right) \tag{5.3}$$

5.5.1 Model validation 7 (PRISME VSP S3)

The initial conditions for the input parameters are listed here (others are similar to what appear in Section 5.3.2):

$N = 0.016,\ \tau = 80$ s
$\overline{\mathrm{MFR}_{\mathrm{adm}}} = 0.48$ kg/s
$\overline{\mathrm{MLR}} = 0.01$ kg/s
$t\_\mathrm{switch} = 180$ s

where the values of $\overline{\mathrm{MFR}_{\mathrm{adm}}}$, $\overline{\mathrm{MLR}}$ and t_switch can similarly be observed from the simulation plots by setting $N = 0$.

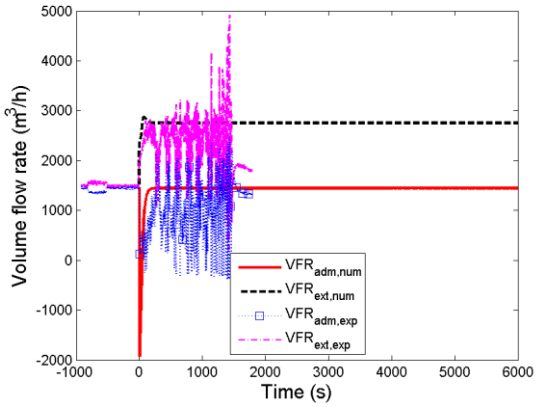

Figure 5-48 Time variation of volume flow rate a validation test of coupling admission flow rate with mass loss rate (PRISME VSP S3, N=0)

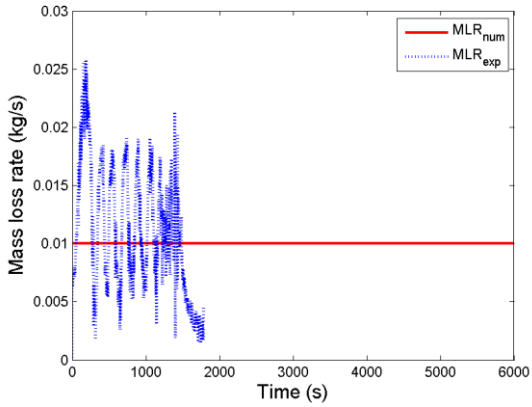

Figure 5-49 Time variation of mass loss rate, a validation test of coupling admission flow rate with mass loss rate (PRISME VSP S3, N=0)

The output plots for the case when $N = 0.016$ are listed as below:

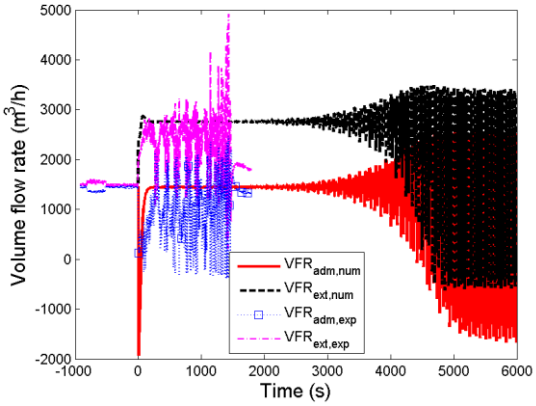

Figure 5-50 Time variation of volume flow rate, a validation test of coupling admission flow rate with mass loss rate (PRISME VSP S3)

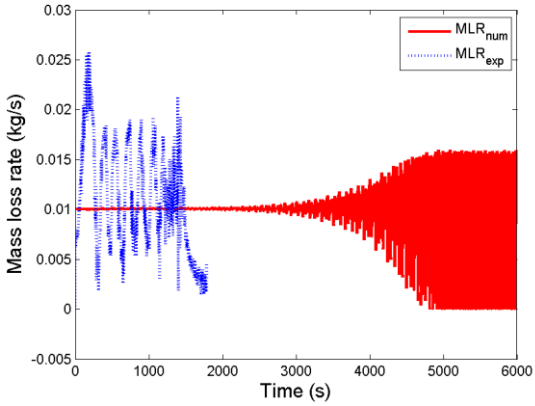

Figure 5-51 Time variation of mass loss rate, a validation test of coupling admission flow rate with mass loss rate (PRISME VSP S3)

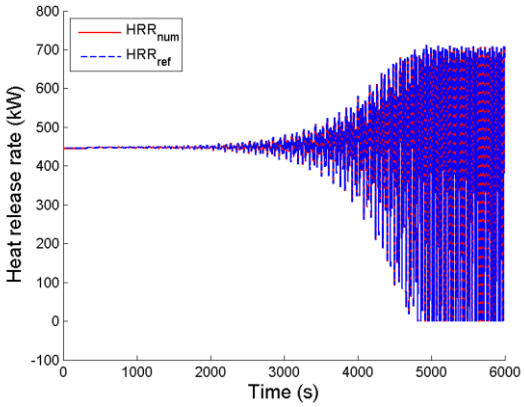

Figure 5-52 Time variation of heat release rate, a validation test of coupling admission flow rate with mass loss rate (PRISME VSP S3)

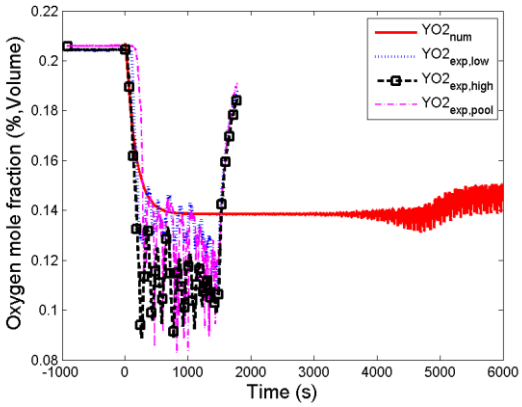

Figure 5-53 Time variation of oxygen mole fraction, a validation test of coupling admission flow rate with mass loss rate (PRISME VSP S3)

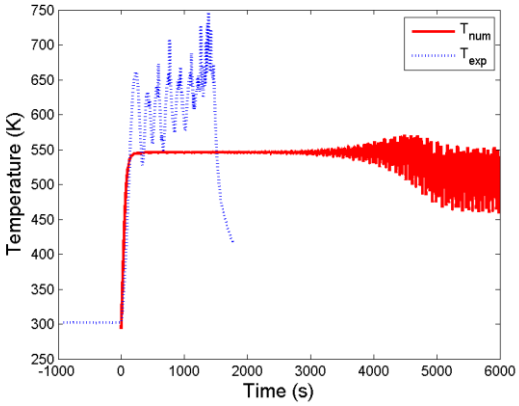

Figure 5-54 Time variation of temperature, a validation test of coupling admission flow rate with mass loss rate (PRISME VSP S3)

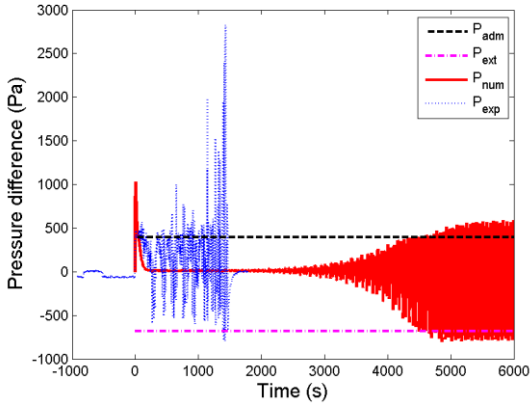

Figure 5-55 Time variation of pressure, a validation test of coupling admission flow rate with mass loss rate (PRISME VSP S3)

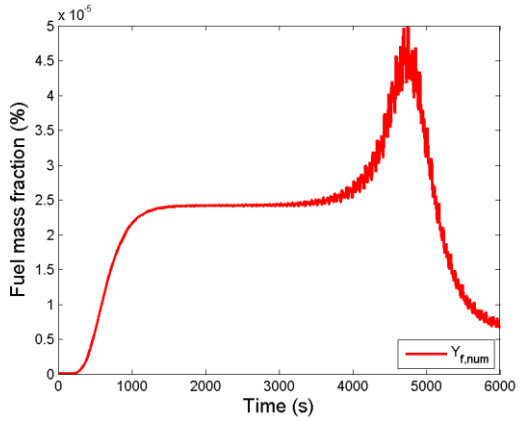

Figure 5-56 Time variation of fuel mass fraction, a validation test of coupling admission flow rate with mass loss rate (PRISME VSP S3)

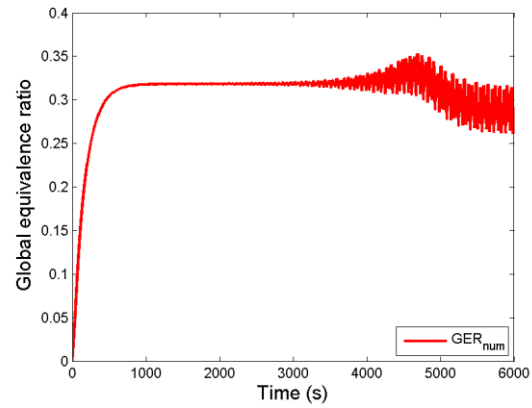

Figure 5-57 Time variation of global equivalence ratio, a validation test of coupling admission flow rate with mass loss rate (PRISME VSP S3)

During this coupling, it is noticeable that the amplitudes of the oscillations may match well with the experimental plots; however, the periods of the numerical plots are so small compared to the experimental ones. This might be because of the characteristic differences between flow rate and oxygen mass fraction or temperature. For instance, a flow rate may vary a lot in a short time; however, the variations of oxygen fraction and temperature cannot be that large. Therefore, the codes for the coupling need to be modified before further oscillation study.

5.6 Oscillation analysis

In this section, according to the validations above, only groups of typical N-τ values from Section 5.3 –the coupling of oxygen mass fraction with mass loss rate- are selected. Their frequencies and amplitudes are recorded for oscillation analysis.

Generally, there are three typical types of oscillation plots. Take the cases in Section 5.3.2 (PRISME VSP S3 package) as examples:

5.6.1 Stable system

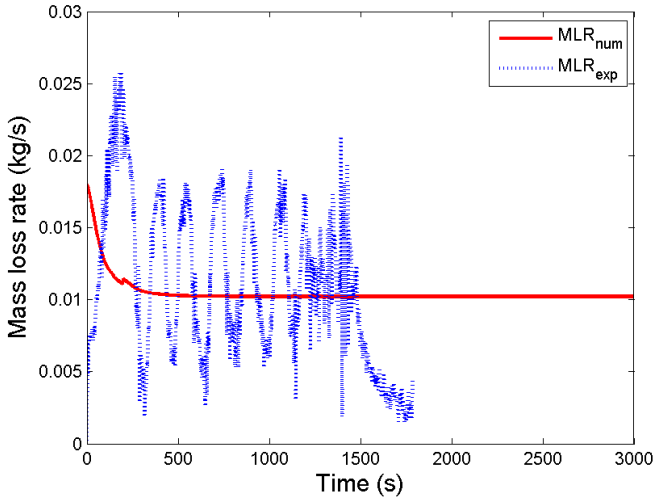

Figure 5-58 Time variation of mass loss rate, a validation test of coupling oxygen fraction with mass loss rate (PRISME VSP S3, N=0.1, τ=40 s)

In Figure 5-58, 3000 s is selected to be the simulation time. However, during this time, there is no obvious oscillation in the plot; in addition, even the 'findpeaks' function in Matlab cannot work here. Therefore, it is hard to detect both the frequency and the amplitude in this case, and their values can just be assumed to be 0.

5.6.2 Unstable system with steady state

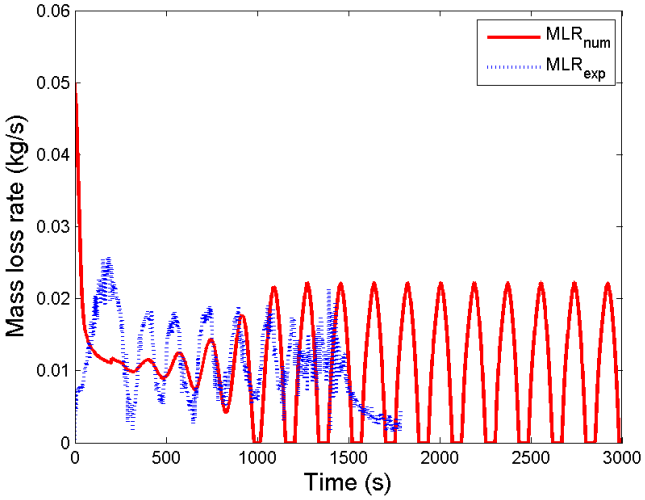

Figure 5-59 Time variation of mass loss rate, a validation test of coupling oxygen fraction with mass loss rate (PRISME VSP S3, N=0.5, τ=60 s)

In Figure 5-59, 3000 s is set to be the simulation time, and 1780 s is set to be the experimental time. Before 1780 s, there are obvious oscillations in the plot. Meanwhile, the amplitude and frequency of these fluctuations are stable and continuing. Therefore, it is considered to be an unstable system with steady state, and its exact values of the amplitude and frequency are necessary to be recorded.

5.6.3 Unstable system without steady state

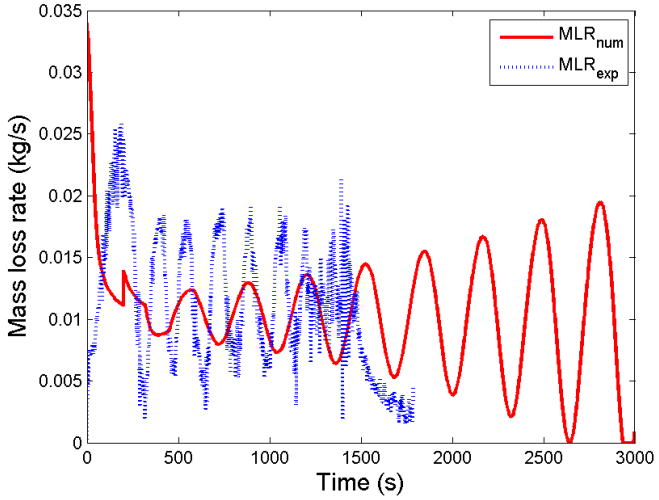

Figure 5-60 Time variation of mass loss rate, a validation test of coupling oxygen fraction with mass loss rate (PRISME VSP S3, N=0.3, τ=120 s, t=3000 s)

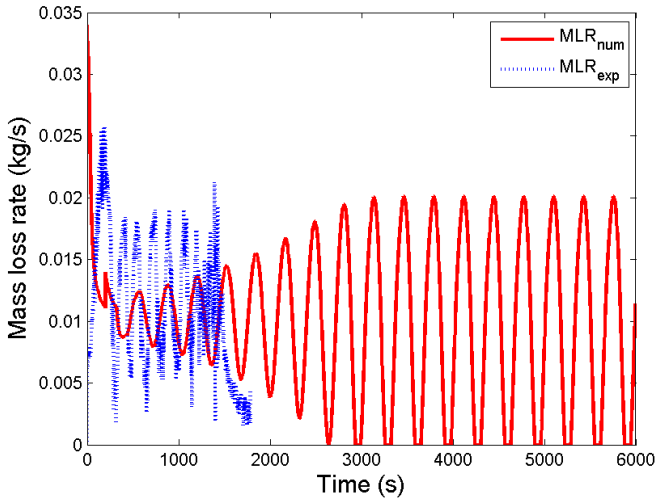

Figure 5-61 Time variation of mass loss rate, a validation test of coupling oxygen fraction with mass loss rate (PRISME VSP S3, N=0.3, τ=120 s, t=3000 s)

In Figure 5-60, 3000 s is chosen to be the simulation time, and 1780 s is the experimental time. Before 1780 s, though there are obvious oscillations in the plot, they are not stable even at 3000 s.

In Figure 5-61, 6000 s instead of 3000 s is set to be the simulation time. The steady state of the oscillation can be observed around 3500 s here. Therefore, it is considered to be an unstable system without steady state, and the values of the amplitude and period should be directly recorded.

5.6.4 Analysis of amplitudes and periods (PRISME Source D1)

The data for the plots here are collected from 140 groups of typical coupling of oxygen fraction with mass loss rate by using N-τ model and PRISME Source D1 package. Function 'contourf' in Matlab is used to draw the contour plots below:

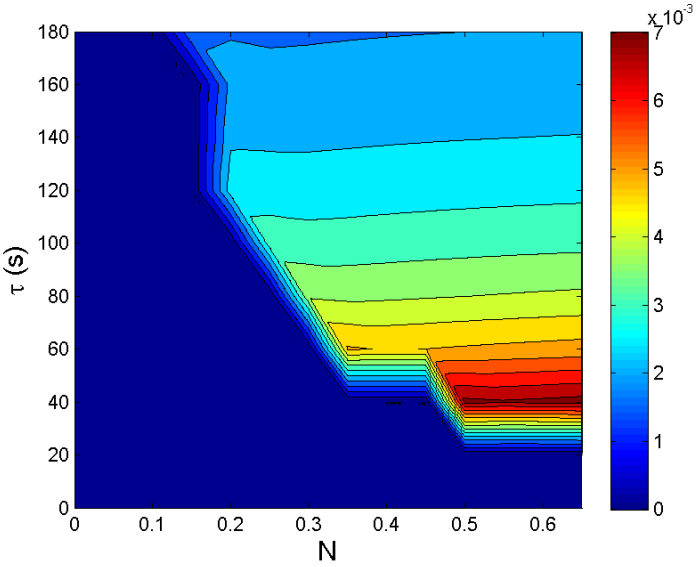

Figure 5-62 Frequency variations with various N and τ, validation tests of coupling oxygen fraction with mass loss rate (PRISME Source D1)

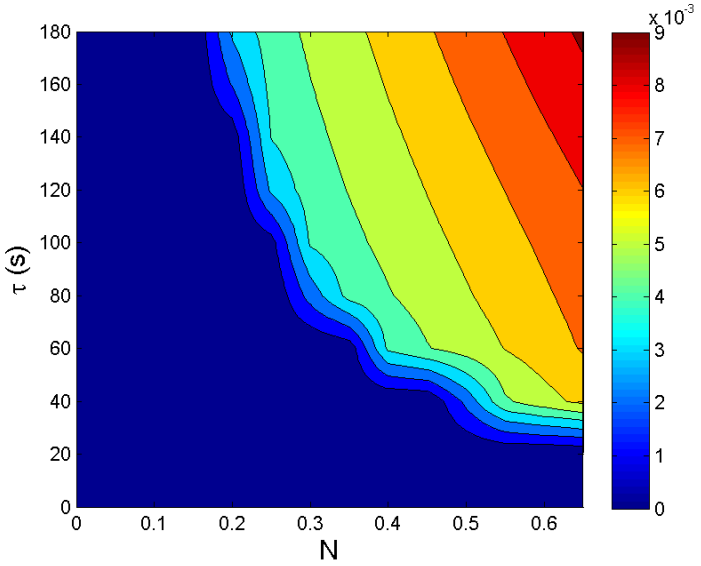

Figure 5-63 Amplitude variations with various N and τ, validation tests of coupling oxygen fraction with mass loss rate (PRISME Source D1)

From Figure 5-62 and 5-63, the value of the frequency increases as N increases and τ decreases; the value of the amplitude is proportional to the values of N and τ. Both two figures share a similar comparatively stable area. To note, when the value of mass loss rate is less than 10^{-5}, which is around 2‰ of the value of mass loss rate observed from the experimental plot, its values of frequency and amplitude are both considered to be 0.

5.6.5 Analysis of amplitudes and periods (PRISME VSP S3)

The data for the plots here are collected from 138 groups of typical coupling of oxygen fraction with mass loss rate by using N-τ model and PRISME VSP S3 package. Function ‘contourf’ in Matlab is also used to draw the contour plots below:

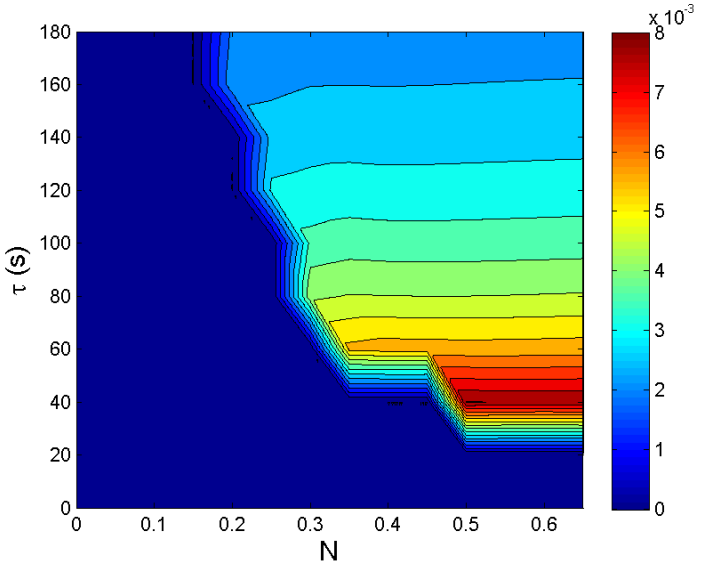

Figure 5-64 Frequency variations with various N and τ, validation tests of coupling oxygen fraction with mass loss rate (PRISME VSP S3)

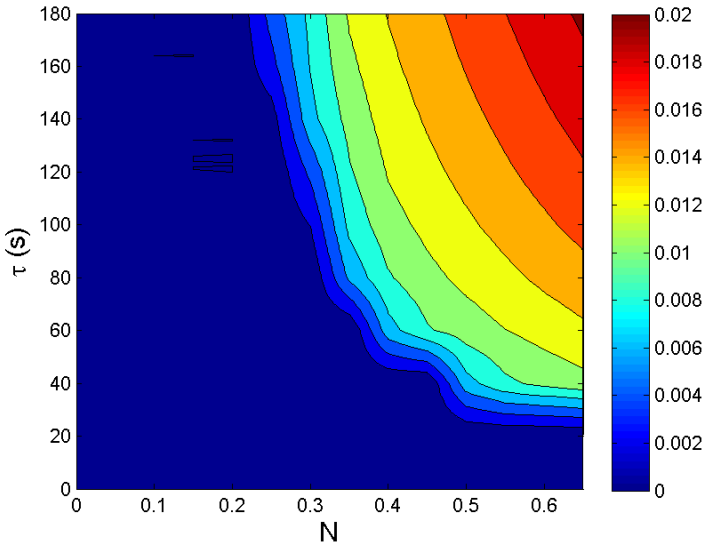

Figure 5-65 Amplitude variations with various N and τ, validation tests of coupling oxygen fraction with mass loss rate (PRISME VSP S3)

Similarly to the section above, in Figure 5-64 and 5-65, the value of the frequency increases as N increases and τ decreases; the value of the amplitude is proportional to the values of N and τ. Both two figures share a similar area of the comparatively stable area. To note, when the value of mass loss rate is less than 10^{-5},

which is 1‰ of the value of mass loss rate observed from the experimental plot, the values of the frequency and amplitude are both considered to be 0.

It is noticeable that the plots here share a similar area division with those in Section 5.6.4 above. However, a smaller stable area is expected for the plots here since the fluctuations of the original experimental plots are tiny in the previous case. Besides, the maximum value of the amplitude on the color bar is larger here; the maximum value of the period range on the color bar is similar. The ratio of the maximum values of the amplitude is reasonable, since it is almost proportional to that of the average values of the experimental mass loss rates.

5.7 Conclusion

In this chapter, the instability behavior of a compartment fire is studied. The coupling of the oxygen mass fraction with the mass loss rate by applying N-τ method is overall reasonable; especially in the validation by using PRISME VSP S3 data package. However, more experimental data is required for further oscillation study. Meanwhile, it is necessary to develop the model for a more universal use, for example, to fix the problems happen to the comparatively steady mass loss rate scenario. Furthermore, the oscillation analyses shall be applied to more types of couplings (for example, the coupling of temperature and admission flow rate mentioned above) after the problems in the basic models are corrected.

6 Conclusions and future work

This research is to study the unstable behavior in a compartment fire. The simulation model is established to understand the coupling between pyrolysis, combustion, pressure and ventilation leading to the unstable behavior. The model is tested by series of verification tests and then validated by comparisons with data collected from PRISM experiments.

The first step is to build a preliminary structure to test the environment parameters, for example, pressure, temperature, mass loss rate, etc., by using seven corresponding ordinary differential equations. The second step is to apply Bernoulli's method to check the stability of the system, and then to confirm it by using a designed mass loss rate (both over-ventilation and under-ventilation regimes are considered). After that, Helmholtz's theory is used to check the proposed oscillation, and the data from PRISM VSP experiments are used to validate the model. The last step is to create a mass loss rate input and therefore to study the frequency and period of the oscillations.

During the study, the flame extinction is considered in this simulation model to ensure the reasonability. The tests successfully verify the proposed stability and oscillations in the preliminary tests. Meanwhile, by using prescribed mass loss rate inputs, the curves plotted by the numerical model match well with those plotted by the experimental data. After that, a detailed oscillation study on the coupling of three environmental parameters with mass loss rate is performed, the detailed analyses and results are elaborated in chapter 5.

The coupling of oxygen mass fraction with mass loss rate (unstable) performs the best during the validation, due to the formulation is most successful at revealing oscillations that consistent with experimental observations. However, the models do not performing well when coupling the mass loss rate with temperature, admission air flow, etc.; therefore the model needs to be improved for a wider use and other types of couplings will be considered next.

Furthermore, though the coupling is successful when choosing a suitable N and τ, N and τ themselves cannot be predicted without numerous trials. Therefore, a more complete model with the prediction of N and τ is required.

Bibliography

[1] Quintiere, J.G. "Fire behavior in building compartments." Proceedings of the combustion institute 29.1 (2002): 181-193.

[2] Spearpoint, M., Mowrer, F.W. and McGrattan, K. "Simulation of a compartment flashover fire using hand calculations, zone models and a field model." Proceedings of the Third International Conference on Fire Research and Engineering (ICFRE3). 1999.

[3] Quintiere, J.G. *Fundamentals of fire phenomena*. Wiley, 2006.

[4] Peatross, M.J. and Beyler, C.L. "Ventilation effects on compartment fire characterization." Fire Safety Science 5 (1997): 403-414.

[5] Hu, Z., Utiskul, Y., Quintiere, J.G. and Trouvé, A. "A comparison between observed and simulated flame structures in poorly ventilated compartment fires." Fire Safety Science 8 (2005): 1193-1204.

[6] https://en.wikipedia.org/wiki/Air%E2%80%93fuel_ratio

[7] Andersson, B., Holmstedt, G. and Dagneryd, A. "Determination of the equivalence ratio during fire, comparison of techniques." Fire Safety Science 7 (2003): 295-308.

[8] http://www.power-eng.com/articles/print/volume-119/issue-1/features/the-use-of-natural-ventilation-for-power-plants.html

[9] Hosser, D. and Volker H. "Application of a new model for the simulation of coupled heat transfer processes during fires to safety relevant objects in nuclear facilities." Fire Safety Journal 62 (2013): 144-160.

[10] Audouin, L., Rigollet, L., Prétrel, H., Le Saux, W. and Röwekamp, M. "OECD PRISME project: Fires in confined and ventilated nuclear-type multi-compartments-Overview and main experimental results." Fire Safety Journal 62 (2013): 80-101.

[11] Sugawa, O., Kawagoe, K., Oka, Y. and Ogahara, I. "Burning behavior in a poorly-ventilated compartment fire-ghosting fire." Fire Science and Technology 9.2 (1989): 2_5-2_14.

[12] Utiskul, Y., Quintiere, J.G., Rangwala, A.S., Ringwelski, B.A, Wakatsukiet, K. and Naruse, T. "Compartment fire phenomena under limited ventilation." Fire Safety Journal 40.4 (2005): 367-390.

[13] Hurley, M.J., Gottuk, D.T., Hall Jr., J. R., Kazunori, H., Kuligowski, E.D., Puchovsky, M., Torero, J., Watts Jr., J.M., and Wieczorek, C.J., eds. *SFPE handbook of fire protection engineering*. Springer, 2015.

[14] https://en.wikipedia.org/wiki/Mechanical_ventilation

[15] Iqbal, N., and Salley, M.H. "Fire Dynamics Tools." Division of System Safety and Analysis Office of Nuclear Reactor Regulation, US Nuclear Regulatory Commission (2004).

[16] Takeda, H., and Akita, K. "Critical phenomenon in compartment fires with liquid fuels." Symposium (International) on Combustion. Vol. 18. No. 1. Elsevier, 1981.

[17] Tewarson, A. "Some observations on experimental fires in enclosures, part II-Ethyl alcohol and paraffin oil." Combustion and Flame 19.3 (1972): 363-371.

[18] Kim, K.I., Ohtani, H., and Uehara, Y. "Experimental study on oscillating behaviour in a small-scale compartment fire." Fire safety journal 20.4 (1993): 377-384.

[19] Prétrel, H., Querre, P. and Forestier, M. "Experimental study of burning rate behavior in confined and ventilated fire compartments." Fire Safety Science 8 (2005): 1217-1228.

[20] Prétrel, H., and Such, J.M. "Effect of ventilation procedures on the behaviour of a fire compartment scenario." Nuclear engineering and design 235.20 (2005): 2155-2169.

[21] Le Saux, W., Prétrel, H., Lucchesi, C. and Guillou, P. "Experimental study of the fire mass loss rate in confined and mechanically ventilated multi-room scenarios." Fire Safety Science 9 (2008): 943-954.

[22] Bonte, F., Noterman, N. and Merci B. "Computer simulations to study interaction between burning rates and pressure variations in confined enclosure fires." Fire Safety Journal 62 (2013): 125-143.

[23] Audouin, L., Chandra, L., Consalvi, J.-L., Gay, L., Gorza, E., Hohm, V., Hostikka, S., Ito, T., Klein-Hessling,W., Lallemand, C., Magnusson, T., Noterman, N., Park, J.S., Peco, J., Rigollet, L., Suard, S. and Van-Hees, P. "Quantifying differences between computational results and measurements in the case of a large-scale well-confined fire scenario." Nuclear Engineering and Design 241.1 (2011): 18-31.

[24] Crocco, L. "Aspects of combustion stability in liquid propellant rocket motors part I: fundamentals. Low frequency instability with monopropellants." Journal of the American Rocket Society 21.6 (1951): 163-178.

[25] Crocco, L. "Aspects of Combustion Stability in Liquid Propellant Rocket Motors Part II: Low Frequency Instability with Bipropellants. High Frequency Instability." Journal of the American Rocket Society 22.1 (1952): 7-16.